# Resonant multiple wave scattering in the seismic response of a city

Geert Lombaert, Didier Clouteau

# Resonant multiple wave scattering in the seismic response of a city

G. Lombaert†* and D. Clouteau‡

†Postdoctoral Fellow of the Fund for Scientific Research-Flanders, K.U. Leuven, Department of Civil Engineering, Kasteelpark Arenberg 40, B-3001 Leuven, Belgium
‡Ecole Centrale Paris, Laboratoire des Sols, Structures et Matériaux, Grande Voie des Vignes, F-92295 Châtenay-Malabry Cedex, France

When a seismic wavefield impinges on the foundation of a building, the building vibrates and gen-erates waves in the subsoil. In a city, different buildings interact with each other through the scat-tered waves. The detailed description of the wave propagation in this coupled city–soil system is a complex problem. Instead of solving this problem for a particular city configuration, a statistical description of the city is applied and the limit of a city of infinite size is considered. This leads to a model of the coupled city–soil system, where the buildings are modelled as resonant scatterers that are uniformly distributed at the surface of a deterministic, horizontally layered elastic half-space that represents the soil. The equations that govern the interaction between the city and the soil now become a set of stochastic equations. Based on these equations, the Dyson and Bethe–Salpeter for the configurationally averaged field and field correlation are formulated. The solution of the sin-gle scatterer problem is used to obtain an approximate solution of these equations that allows us to quantify the change of the mean site response through the presence of the city and the ratio of the coherent and incoherent response. Furthermore, the influence of the city on the duration of the seismic records is estimated by the approximate solution of the non-stationary Bethe–Salpeter equation. The results obtained for the configurationally averaged field quantities are validated by means of results for the seismic response of a deterministic model of a city quarter of Mexico City.

## 1. Introduction

Seismic records from dense urban arrays have shown a large dispersion attributed to highly varying local site conditions around stations [1]. Furthermore, seismic records from the lake bed of Mexico City are characterized by a long duration and beating phenomena [2]. For the case of the September 1985 Michoacan earthquake in Mexico City, Chavez-Garcia and Bard [1] have critically reviewed some of the models proposed to explain the observed site response. Although most of these models account for the spatial variability of the soil response, the large duration remains unexplained. In order to more satisfactorily explain the features of these seismic records, several authors have investigated the influence of the presence of the city on the seismic site response.

*Corresponding author. E-mail: geert.lombaert@bwk.kuleuven.be

Wirgin and Bard [3] were among the first to propose a numerical model for the quantification of the city-site effect. Clouteau and Aubry [4] have applied a periodic city model, where the periodicity is assumed to be much larger than the correlation length. Guéguen et al. [5] have used an independent scattering approximation to estimate the city-site effect for a group of 180 buildings of the Roma Norte quarter of Mexico City. Mezher et al. [6] and Mezher [7] have performed calculations that fully account for the multiple wave scattering between the buildings for a group of 77 buildings of the same quarter. Tsogka and Wirgin [8] and Groby et al. [9] have studied a 2D model with 10 buildings without [8] and with [9] internal energy dissipation. Boutin and Roussillon [10] have proposed a simplified analytical procedure, where the presence of the city on the site is modelled by means of an equivalent layer.

A seismic wavefield excites the buildings in the city that will interact with each other through the scattered waves. The city-site effect is therefore a problem of multiple wave scattering by discrete scatterers, as considered by Foldy [11] and discussed extensively by Waterman and Truell [12]. Moreover, as the incident wavefield excites the buildings in the frequency range of their resonance frequencies, it is a case of resonant multiple wave scattering [13]. Instead of solving this complex problem for a particular city configuration, a statistical model of the city is applied and the limit of a city of infinite size is considered within the frame of the present paper.

The city is modelled as a collection of resonant finite size scatterers, uniformly distributed at the soil's surface, which is represented by a horizontally layered elastic half-space. This leads to a set of stochastic equations that governs the interaction between the city and the soil. From these equations, the Dyson and Bethe–Salpeter equations [14–17] for the configurationally averaged field and field correlation are derived in a similar way as done by Weaver [18, 19] for the interaction of a plate with a set of randomly distributed single degree of freedom systems. The solution of the single scatterer problem is used to obtain an approximate solution of these equations that allows us to quantify the city-site effect in terms of the mean field and the dispersion around the mean site response. The solution of the non-stationary Bethe–Salpeter equation allows us to verify whether the presence of the city increases the duration of the seismic site response.

The results are validated by means of numerical results obtained by Mezher et al. [6] from a deterministic analysis of the response of a complete city quarter of the Roma Norte district of Mexico City.

## 2. The governing equations of motion

### 2.1 *The soil domain*

The soil domain is modelled as an elastic, horizontally layered half-space, denoted by $D$ (figure 1). The soil's boundary $\partial D$ consists of the surface $S$ at $z = 0$ and the boundary $S_\infty$ at infinity. The city is modelled as a collection of oscillators, uniformly distributed over the soil's surface $S$. The interface between the buildings and the soil is denoted by $\Gamma$ and consists of the union $\cup\Gamma_j$ of all interfaces $\Gamma_j$ between a building $j$ and the soil. The soil's traction free surface $S_f$ is found as $S\backslash\Gamma$. In the following, we will derive the equations that govern the interaction between the city and the soil for an incident wavefield $\mathbf{u}_i$. The latter is the wavefield in the soil when no buildings are present.

The total displacement field $\mathbf{u}$ in the soil has to satisfy the following homogeneous Navier equations of motion in the frequency domain:

$$-\mathrm{div}\boldsymbol{\sigma}(\mathbf{u}) - \rho\omega^2\mathbf{u} = 0 \text{ in } D \tag{1}$$

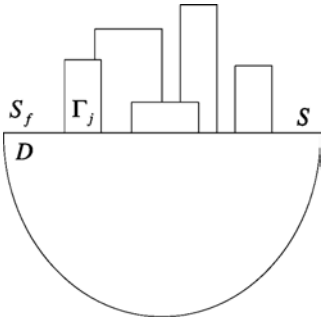


Figure 1. Model of a city interacting with an elastic half-space.

where $\boldsymbol{\sigma}(\mathbf{u})$ is the stress tensor in the soil, which is computed from the strain tensor $\boldsymbol{\epsilon}$ by means of Hooke's law as $\sigma_{ij} = c_{ijkl}\epsilon_{kl}$. For an isotropic elastic material, the Hooke tensor $\mathbf{c}$ depends on the Lamé constants $\lambda$ and $\mu$ only.

The total displacement field $\mathbf{u}$ in the soil domain $\Omega$ is decomposed into the incident wavefield $\mathbf{u}_\mathrm{i}$ and the diffracted wavefield $\mathbf{u}_\mathrm{d}$:

$$\mathbf{u} = \mathbf{u}_\mathrm{i} + \mathbf{u}_\mathrm{d} \tag{2}$$

The incident wavefield $\mathbf{u}_\mathrm{i}$ satisfies the homogeneous Navier equation in $D$ and the traction-free boundary condition at the surface $S$. The diffracted wavefield $\mathbf{u}_\mathrm{d}$ satisfies the homogeneous Navier equation together with the radiation conditions at $S_\infty$, the traction-free boundary conditions at the free surface $S_f$ and the following boundary conditions at each interface $\Gamma_j$ between a building and the soil:

$$\begin{aligned} \mathbf{u}_\mathrm{d} + \mathbf{u}_\mathrm{i} &= \mathbf{u}_{\mathrm{f}j} \quad \text{on } \Gamma_j \\ \mathbf{t}(\mathbf{u}) + \mathbf{t}_{\mathrm{b}j} &= 0 \qquad \text{on } \Gamma_j \end{aligned} \tag{3}$$

where $\mathbf{u}_{\mathrm{f}j}$ represents the foundation displacements of building $j$. The soil tractions $\mathbf{t}(\mathbf{u})$ at the interface are calculated as $\boldsymbol{\sigma}(\mathbf{u})\mathbf{n}$, where $\mathbf{n}$ is the outward unit normal vector to $\Gamma_j$. If all buildings are located at the free surface $S$, $\mathbf{t}(\mathbf{u}_\mathrm{i}) = 0$ on $\Gamma_j$ and therefore $\mathbf{t}(\mathbf{u}) = \mathbf{t}(\mathbf{u}_\mathrm{d})$.

### 2.2 *The building model*

For each building, the building tractions $\mathbf{t}_\mathrm{b}$ are calculated from the interaction forces $\mathbf{F}$ between the building and the soil as:

$$\mathbf{t}_\mathrm{b} = \boldsymbol{\Pi}(\mathbf{x} - \mathbf{x}_\mathrm{b})\mathbf{F} \text{ for } \mathbf{x} \text{ and } \mathbf{x}_\mathrm{b} \text{ on } S \tag{4}$$

where $\boldsymbol{\Pi}(\mathbf{x} - \mathbf{x}_\mathrm{b})$ is a $3 \times 3$ matrix of which each element $\Pi_{kl}$ contains the stress distribution in a direction $\mathbf{e}_k$ due to a unit resultant force in a direction $\mathbf{e}_l$ for a building at a position $\mathbf{x}_b$. In the following, the foundations of all buildings are assumed to be rigid and to have the same size, so that the same matrix $\boldsymbol{\Pi}$ is used for each building.

In the low-frequency range that is relevant in earthquake engineering, the dynamic response of a building in the horizontal direction is satisfactorily modelled by means of a single degree of freedom (DOF) oscillator that takes into account the motion of the building in the first horizontal mode [20]. This leads to a building model, where the building mass $m$ is coupled to a foundation at the soil's surface by means of a spring-damper connection with a dynamic stiffness $k + i\omega c$ in the frequency domain. The interaction force $F_x$ between the building and the soil in the horizontal direction $\mathbf{e}_x$, is calculated from the displacement $u_{\mathrm{b}x}$ of the building

mass and the foundation displacement $u_{\mathrm{f}x}$:

$$F_x = -(k + i\omega c)[u_{\mathrm{b}x} - u_{\mathrm{f}x}] \tag{5}$$

where $k$ denotes the stiffness and $c$ the damping coefficient that determines the internal energy dissipation in the building. The equation of motion of the building is:

$$-(k + i\omega c)[u_{\mathrm{b}x} - u_{\mathrm{f}x}] = -m\omega^2 u_{\mathrm{b}x} \tag{6}$$

The equations of motion are now used to eliminate the building displacements $u_{\mathrm{b}x}$ from equation (5) for the interaction forces. The relation between the force $F_x$ and the displacement $u_{\mathrm{f}x}$ is the building impedance $i\omega Z$ and is rewritten as follows in terms of the resonance frequency $\omega_{\mathrm{res}} = \sqrt{k/m}$ and the damping ratio $\zeta = c/2\sqrt{km}$ of a building fixed at its base:

$$F_x = -m\omega^2 \left( \frac{\omega_{\mathrm{res}}^2 + 2i\zeta\omega_{\mathrm{res}}\omega}{\omega_{\mathrm{res}}^2 + 2i\zeta\omega_{\mathrm{res}}\omega - \omega^2} \right) u_{\mathrm{f}x} \tag{7}$$

As the building mass is distributed along the building height, only about 81% of the entire building mass participates in the first horizontal mode of the structure [20]. This effect can be accounted for replacing the mass $m$ in equation (7) by $0.81m$ and adding an additional term $-0.19m\omega^2 u_{\mathrm{f}x}$ that accounts for the remaining part.

According to the first boundary condition in equation (3), the foundation displacement $u_{\mathrm{f}x}$ can be replaced by the total soil displacement $u_x(\mathbf{x}_{\mathrm{b}})$ at the center of gravity $\mathbf{x}_{\mathrm{b}}$ of the foundation as the foundation is assumed to be rigid and the rocking motion of the buildings is neglected.

In the following, the buildings are assumed to have the same dynamic characteristics in both horizontal directions $\mathbf{e}_x$ and $\mathbf{e}_y$ and the same impedance $i\omega Z$ is used to relate $F_y$ and $u_y(\mathbf{x}_{\mathrm{b}})$ for each building. The vector $\mathbf{F}$ is calculated from the soil displacements $\mathbf{u}(\mathbf{x}_{\mathrm{b}})$ as:

$$\mathbf{F} = i\omega\mathbf{Z}\mathbf{u}(\mathbf{x}_{\mathrm{b}}) \tag{8}$$

where $i\omega\mathbf{Z}$ is a $3 \times 3$ diagonal matrix that contains the horizontal building impedance $i\omega Z$ on its first two diagonal elements.

### 2.3 *The probabilistic city model*

The city is modelled as a limiting large number ($N \to \infty$) of buildings, randomly distributed on the entire soil surface $S$ with a uniform surface density $\rho_{sc}$. If all buildings have the same foundation size $S_b$, the surface density is calculated as $\eta/S_b$, where $\eta$ represents the ratio of the built and total soil surface.

The building resonance frequency $\omega_{\mathrm{res}}$ in equation (7) is modelled as a random variable $\Omega_{\mathrm{res}}$. The resonance frequency and the position of the buildings are assumed to be independent random variables. The eigenfrequency $\omega_{\mathrm{res}}/2\pi$ of a building is approximately inversely proportional to the building height, as indicated by building codes [21], and can be estimated from the number $n$ of floors as $10/n$ [Hz]. The building mass $m$ is estimated from the foundation size and the number of floors and is therefore determined by $\Omega_{\mathrm{res}}$ as well. The damping ratio $\zeta$ is assumed to have the same deterministic value for all buildings, as conventionally given in building codes [21].

### 2.4 *The city–soil interaction*

The second boundary condition in equation (3) can be rewritten by means of the building impedance $i\omega\mathbf{Z}_j$ for each building $j$ as:

$$\boldsymbol{\sigma}(\mathbf{u}_\mathrm{d})\mathbf{n} + \sum_{j=1}^{N} \boldsymbol{\Pi}(\mathbf{x} - \mathbf{x}_{\mathrm{b}j}) i\omega\mathbf{Z}_j \mathbf{u}(\mathbf{x}_{\mathrm{b}j}) = 0 \text{ on } \Gamma = \cup\Gamma_j \tag{9}$$

Equation (9) can be transformed into an integral equation for the diffracted wavefield by means of the representation theorem in elastodynamics:

$$\mathbf{u}_\mathrm{d}(\mathbf{x}) = -\int_S \mathbf{U}^G(\mathbf{x}, \mathbf{x}') \left( \sum_{j=1}^{N} \boldsymbol{\Pi}(\mathbf{x}' - \mathbf{x}_{\mathrm{b}j}) i\omega\mathbf{Z}_j \mathbf{u}(\mathbf{x}_{\mathrm{b}j}) \right) d\mathbf{x}' \tag{10}$$

where $\mathbf{U}^G(\mathbf{x}, \mathbf{x}')$ is the Green's displacement tensor. Each element $U^G_{ij}(\mathbf{x}, \mathbf{x}')$ of the Green's tensor represents the displacement at a position $\mathbf{x}'$ in a direction $\mathbf{e}_j$ due to a unit impulse load at a position $\mathbf{x}$ in a direction $\mathbf{e}_i$. The Green's tensor is used to define the following operator $\mathcal{U}^G$:

$$(\mathcal{U}^G\mathbf{f})(\mathbf{x}) = \int_S \mathbf{U}^G(\mathbf{x}, \mathbf{x}')\mathbf{f}(\mathbf{x}')\, d\mathbf{x}' \tag{11}$$

Equation (2) is used to replace the diffracted wavefield $\mathbf{u}_\mathrm{d}(\mathbf{x})$ by the total wavefield $\mathbf{u}(\mathbf{x})$ minus the incident wavefield $\mathbf{u}_\mathrm{i}(\mathbf{x})$. Furthermore, the displacement $\mathbf{u}(\mathbf{x}_{\mathrm{b}j})$ at $\mathbf{x}_{\mathrm{b}j}$ is rewritten as an integral on the entire surface $S$ of the product of the total wavefield $\mathbf{u}(\mathbf{x})$ and a Dirac delta function that selects the right position $\mathbf{x}_{\mathrm{b}j}$:

$$\mathbf{u}(\mathbf{x}) = \mathbf{u}_\mathrm{i}(\mathbf{x}) - \int_S \mathbf{U}^G(\mathbf{x}, \mathbf{x}') \sum_{j=1}^{N} \boldsymbol{\Pi}(\mathbf{x}' - \mathbf{x}_{\mathrm{b}j}) i\omega\mathbf{Z}_j \int_S \boldsymbol{\delta}(\mathbf{x}'' - \mathbf{x}_{\mathrm{b}j}) \mathbf{u}(\mathbf{x}'')\, d\mathbf{x}''\, d\mathbf{x}' \tag{12}$$

The previous equation (12) is a Lippmann–Schwinger equation and is written in an operator notation as follows:

$$\mathbf{u} = \mathbf{u}_\mathrm{i} - \mathcal{U}^G \Lambda_\delta \mathbf{u} \tag{13}$$

where the operator $\Lambda_\delta$ is given by:

$$(\Lambda_\delta \mathbf{v})(\mathbf{x}') = \sum_{j=1}^{N} \boldsymbol{\Pi}(\mathbf{x}' - \mathbf{x}_{\mathrm{b}j}) i\omega\mathbf{Z}_j \int_S \boldsymbol{\delta}(\mathbf{x}'' - \mathbf{x}_{\mathrm{b}j}) \mathbf{v}(\mathbf{x}'')\, d\mathbf{x}''$$

This operator is referred to as the impurity potential operator [17]. As both the position $\mathbf{x}_{\mathrm{b}j}$ and the eigenfrequency $\Omega_\mathrm{res}$ of each building are modelled as random variables, the operator $\Lambda_\delta$ is a stochastic operator. A solution is obtained through the construction of the scattering operator $\mathcal{T}$ [17], which allows the calculation of the diffracted wavefield $\mathbf{u}_\mathrm{d}$ from the incident wavefield $\mathbf{u}_\mathrm{i}$:

$$\mathbf{u} = \mathbf{u}_\mathrm{i} + \mathcal{U}^G \mathcal{T} \mathbf{u}_\mathrm{i} \tag{14}$$

The construction of the scattering operator in the case of a homogeneous elastic half-space containing a bounded heterogenity is discussed by Savin [22] and Savin and Clouteau [23]. In the following, however, we do not intend to construct the scattering operator $\mathcal{T}$ for a given city configuration. Instead, we will consider a statistical description of the city and calculate approximating solutions for the configurationally averaged field and field correlation, based on the scattering operator $\mathcal{T}$ for a single building. The solution of the single scatterer problem also allows us to calculate the scattering cross-section $\sigma$ of the building and to estimate the mean free path $l$.

## 3. The soil–structure interaction problem for a single building

### 3.1 *The scattering operator for a single building*

In order to solve the soil–structure interaction problem for a single building, the diffracted wavefield $\mathbf{u}_\mathrm{d}$ in equation (2) is further decomposed into the locally diffracted wavefield $\mathbf{u}_{\mathrm{d}0}$ [24], which cancels the incident wavefield at the soil–structure interface $\Gamma$, and the wavefield $\mathbf{u}_{sc}$ radiated by the foundation motion. The radiated wavefield $\mathbf{u}_{sc}$ is further decomposed into a number of radiation modes $\mathbf{u}_{\mathrm{d}m}$ that represent the wavefield scattered in the soil by the $m$-th displacement mode of the interface $\Gamma$. In the present case, only the translational rigid body displacement modes of the foundation are considered:

$$\mathbf{u} = \mathbf{u}_\mathrm{i} + \mathbf{u}_{\mathrm{d}0} + \sum_{m=x,y,z} c_m \mathbf{u}_{\mathrm{d}m} = \mathbf{u}_\mathrm{i} + \mathbf{u}_{\mathrm{d}0} + \mathbf{U}_\mathrm{d}\mathbf{c} \tag{15}$$

where $\mathbf{u}_{\mathrm{d}m}(\mathbf{x}_\mathrm{b}) = \mathbf{e}_m$ and therefore $\mathbf{U}_\mathrm{d}(\mathbf{x}_\mathrm{b}) = \mathbf{I}$. With this particular choice of the interface displacement modes, the generalized coordinates $\mathbf{c}$ are the previously defined foundation displacements $\mathbf{u}_\mathrm{f}$. In the case of a surface foundation and a wavefield $\mathbf{u}_\mathrm{i}$ that is uniform along the interface $\Gamma$, the following matrix equation of motion is derived from the formulation of the traction equilibrium at the interface in the weak sense [24]:

$$[i\omega\mathbf{Z} + \mathbf{K}_\mathrm{s}]\,\mathbf{u}_\mathrm{f} = \mathbf{K}_\mathrm{s}\mathbf{u}_\mathrm{i}(\mathbf{x}_\mathrm{b}) \tag{16}$$

where $i\omega\mathbf{Z}$ is the previously defined building impedance. The soil impedance $\mathbf{K}_\mathrm{s}$ is calculated from the tractions $\mathbf{t}(\mathbf{u}_{\mathrm{d}m})$ for the scattered wavefields $\mathbf{u}_{\mathrm{d}m}$:

$$K_{smn} = \int_\Gamma \mathbf{t}(\mathbf{u}_{\mathrm{d}n}) \cdot \mathbf{u}_{\mathrm{d}m}\, d\mathbf{x} \tag{17}$$

When only translational rigid body modes of the foundation are considered, the soil impedance $\mathbf{K}_\mathrm{s}$ is diagonal. The total matrix $[i\omega\mathbf{Z} + \mathbf{K}_\mathrm{s}]$ in equation (16) is diagonal as well, and the displacements $u_{\mathrm{f}m}$ in different directions $\mathbf{e}_m$ decouple. The solution of equation (16) allows us to calculate the forces $\mathbf{F}$ from the incident wavefield $\mathbf{u}_\mathrm{i}$ by means of equation (8):

$$\mathbf{F} = i\omega\mathbf{Z}\,[i\omega\mathbf{Z} + \mathbf{K}_\mathrm{s}]^{-1}\,\mathbf{K}_\mathrm{s}\mathbf{u}_\mathrm{i}(\mathbf{x}_\mathrm{b}) = i\omega\mathbf{Z}'\mathbf{u}_\mathrm{i}(\mathbf{x}_\mathrm{b}) \tag{18}$$

where $i\omega\mathbf{Z}'$ denotes the modified impedance. In the case where the internal damping ratio $\zeta$ is zero, the modified horizontal impedance $i\omega Z'$ can be rewritten in terms of the resonance frequency $\omega_\mathrm{ssi}$ of the building coupled to the soil and the damping ratio $\zeta_\mathrm{ssi}$ that only accounts for radiation and material damping in the soil:

$$F_x = -m\omega^2\left[\frac{\omega_\mathrm{ssi}^2 + 2i\zeta_\mathrm{ssi}\omega_\mathrm{ssi}\omega}{\omega_\mathrm{ssi}^2 + 2i\zeta_\mathrm{ssi}\omega_\mathrm{ssi}\omega - \omega^2\left(1 + 2i\zeta_\mathrm{ssi}\frac{\omega_\mathrm{ssi}\omega}{\omega_j^2}\right)}\right] u_{\mathrm{i}x}(\mathbf{x}_\mathrm{b}) \tag{19}$$

where $\omega_\mathrm{ssi}$ and $\zeta_\mathrm{ssi}$ are calculated from the building mass $m$ and stiffness $k$ and the soil impedance $K_{\mathrm{s}xx}$ that is rewritten as $k_\mathrm{s} + i\omega c_s$:

$$\omega_\mathrm{ssi}^2 = \frac{k k_\mathrm{s}}{m(k + k_\mathrm{s})},\quad \zeta_\mathrm{ssi} = \frac{\omega_\mathrm{ssi} c_s}{2k_\mathrm{s}} \tag{20}$$

Accounting for soil–structure interaction shifts the building resonance frequency $\omega_\mathrm{res}$ to a slightly lower value $\omega_\mathrm{ssi}$ and introduces an energy dissipation due to radiation and material damping in the soil.

Equation (18) for the force $\mathbf{F}$ allows us to calculate the building tractions at the interface by means of equation (4). The total wavefield $\mathbf{u}$ in the entire soil domain $D$ is now calculated

from the incident wavefield $\mathbf{u}_\mathrm{i}$:

$$\mathbf{u} = \mathbf{u}_\mathrm{i} - \mathcal{U}^G \mathbf{\Pi}(\mathbf{x} - \mathbf{x}_\mathrm{b}) i\omega \mathbf{Z}' \mathbf{u}_\mathrm{i}(\mathbf{x}_\mathrm{b}) \tag{21}$$

This identifies the scattering operator $\mathcal{T}$ [17] for a single building as:

$$\left(\mathcal{T}_j \mathbf{v}\right)(\mathbf{x}) = -\mathbf{\Pi}(\mathbf{x} - \mathbf{x}_\mathrm{b}) \int_S i\omega \mathbf{Z}'_j \boldsymbol{\delta}(\mathbf{x}' - \mathbf{x}_\mathrm{b}) \mathbf{v}(\mathbf{x}')\, d\mathbf{x}' \tag{22}$$

In the following, this scattering operator will also be used in the case where the wavefield $\mathbf{u}_\mathrm{i}$ is not uniform along the interface. This implies that the kinematic interaction between the foundation and the incident wavefield is neglected.

### 3.2 *The scattering cross-section of a single building*

The solution of the single scatterer problem allows us to calculate the scattering cross-section of a building. In the independent scattering approximation, this scattering cross-section can be used to estimate the mean free path.

The scattering cross-section is estimated under the hypothesis of Rayleigh scattering of surface waves by means of the optical theorem. The total scattering cross-section $\sigma$ is expressed as the ratio of the power $P_\mathrm{out}$ lost both by absorption and scattering and the power density $p_\mathrm{i}$ of the incident field. As recalled in appendix A, the general form of $P_\mathrm{out}$ for any obstacle of boundary $\Gamma$ embedded in a purely elastic medium is given by:

$$P_\mathrm{out} = \omega \Im\left( \int_\Gamma [\mathbf{t}(\mathbf{u}_\mathrm{d}) \cdot \mathbf{u}_\mathrm{i}{}^* - \mathbf{u}_\mathrm{d} \cdot \mathbf{t}(\mathbf{u}_\mathrm{i})^*] dS \right) \tag{23}$$

where a superscript $^*$ denotes the complex conjugate. Since, for a superficial foundation, $\mathbf{t}(\mathbf{u}_\mathrm{i}) = 0$ and assuming that the foundation size is small compared to the wavelength, the power $P_\mathrm{out}$ is calculated as:

$$P_\mathrm{out} = \omega \Im(\mathbf{F} \cdot \mathbf{u}_\mathrm{i}{}^*) \qquad \mathbf{F} = \int_\Gamma \mathbf{t}(\mathbf{u}) dS \tag{24}$$

where $\mathbf{F}$ is the previously defined interaction force. Equations (18) and (19) are used to calculate the total scattering cross-section as a function of the incident wavefield $\mathbf{u}_\mathrm{i}$ as:

$$\sigma = \frac{P_\mathrm{out}}{p_\mathrm{i}} = \frac{1}{z_\mathrm{i}} \omega^4 \frac{2m\zeta_\mathrm{ssi}\omega_\mathrm{ssi}\alpha}{\left(\omega_\mathrm{ssi}^2 - \omega^2\right)^2 + 4\zeta_\mathrm{ssi}^2 \omega_\mathrm{ssi}^2 \omega^2 \alpha^2} \qquad p_\mathrm{i} = \omega^2 z_\mathrm{i} \|\mathbf{u}_\mathrm{i}\|^2 \tag{25}$$

where $\alpha$ is the ratio $k/(k + k_\mathrm{s})$. For $\omega \ll \omega_\mathrm{ssi}$, the limiting value of the scattering cross-section scales as $\omega^4$ as for the classical Rayleigh scattering limit. For $\omega_\mathrm{ssi} \ll \omega$, the limiting value satisfies $z_\mathrm{i}\sigma \approx 2m\zeta_\mathrm{ssi}\omega_\mathrm{ssi}\alpha$, but this limit is relevant only for vertically incident plane waves since $\mathbf{u}_i$ has to be uniform on the foundation as stated in equation (24). In this particular case, $z_\mathrm{i} = \rho c_s$ and it can be shown from the classical limit of the foundation impedance that $2m\zeta_\mathrm{ssi}\omega_\mathrm{ssi}\alpha = \rho c_s S$ with $S$ the surface of the foundation and therefore $\sigma = S$ as in the high frequency limit of the cross-section of an absorbing obstacle.

The most relevant approximation in our case is, however, for $\omega$ equal to $\omega_\mathrm{ssi}$ leading to a total cross-section inversely proportional to the damping ratio:

$$\sigma z_\mathrm{i} \approx \frac{m\omega_\mathrm{ssi}}{2\zeta_\mathrm{ssi}\alpha} \tag{26}$$

As the damping ratio $\zeta_\mathrm{ssi}$ is usually small, this expression indicates a potential high value for the total cross-section of resonating buildings.

### 3.3 *The mean free path for a uniform distribution of buildings*

In order to compute the total cross-section from equation (26), the normalizing constant $z_i$ has to be determined. The multiple scattering in the city is governed by surface waves and the normalizing constant is therefore of the following form:

$$z_i = \rho c_{\text{surf}} h_{\text{surf}} \tag{27}$$

with $c_{\text{surf}}$ the surface wave velocity and $h_{\text{surf}}$ the depth of the surface wave. The two types of surface wave of interest for a layered half-space are Rayleigh waves on one hand and Love waves on the other. For both types of wave, the wave velocity is of the order of the shear wave velocity of the first layer. The depth $h_{\text{surf}}$ is equal to half the wavelength for Rayleigh waves and equal to the thickness of the first layer for Love waves. For $\omega$ equal to $\omega_{\text{ssi}}$, this leads to the following scattering cross-section:

$$\sigma = \frac{m\omega_{\text{ssi}}}{2\zeta_{\text{ssi}}\alpha\rho c_{\text{surf}} h_{\text{surf}}} \tag{28}$$

In the independent scattering approximation, the mean free path is estimated as $1/\rho_{sc}\sigma$ and, normalized by the wavelength $\lambda = 2\pi c_{\text{surf}}/\omega$, is given by:

$$\frac{l}{\lambda} = \frac{\zeta_{\text{ssi}}\alpha}{\pi}\frac{\rho h_{\text{surf}}}{\gamma\rho_{sc} m} \tag{29}$$

where the surface density $\rho_{sc}$ has been multiplied by the fraction $\gamma$ of buildings that have their resonance frequency $\omega_{\text{ssi}}$ at $\omega$. The second factor in equation (29) represents the ratio of the mass of the mobilized soil and the uniformly distributed mass of the buildings with a resonance frequency $\omega_{\text{ssi}} = \omega$. In the following, the case of Mexico city is considered, where the subsoil is characterized by a weak top layer with a thickness of about 50 m and a density $\rho$ of 1250 kg/m$^3$. The distributed mass of the buildings is calculated from a surface density $\rho_{sc}$ of $5.1 \times 10^{-4}$ m$^{-2}$, with a fraction $\gamma$ equal to 20% for buildings with 10 storeys and an estimated mass per unit surface of 9000 kg/m$^2$ for this type of building. This leads to an estimated value of 109 for the second factor, which is divided by $\pi$ and multiplied by the small damping ratio $\zeta_{\text{ssi}}$ and the factor $\alpha = k/(k + k_{\text{s}})$, which is necessarily smaller than 1. This results in a potentially small ratio of the mean free path and the wavelength $\lambda$ and indicates that multiple wave scattering is of importance in the frequency range of the building resonance frequencies.

## 4. The mean field

### 4.1 *The Dyson equation*

Following the formalism introduced by Frisch [14], the averaging operation is represented by the operator $P$. Applying the operators $P$ and $(I - P)$ on equation (13) allows us to derive the following system of equations for the mean, coherent field $\underline{\mathbf{u}}$ and the incoherent field $\mathbf{u}_f$:

$$\begin{aligned} \underline{\mathbf{u}} &= \mathbf{u}_{\text{i}} - \mathcal{U}^G P \Lambda_\delta(\underline{\mathbf{u}} + \mathbf{u}_f) \\ \mathbf{u}_f &= -\mathcal{U}^G (I - P)\Lambda_\delta(\underline{\mathbf{u}} + \mathbf{u}_f) \end{aligned} \tag{30}$$

The second equation is used to express the incoherent field $\mathbf{u}_f$ as a function of the coherent field by means of a Neumann expansion for the inverse of the operator $I + \mathcal{U}^G(I - P)\Lambda_\delta$. Introducing this expression in the first equation results in the Dyson equation [14] for the

mean field:

$$\underline{\mathbf{u}} = \mathbf{u}_\mathrm{i} + \mathcal{U}^G \mathcal{M} \underline{\mathbf{u}} \tag{31}$$

where $\mathcal{M}$ represents the mass operator:

$$\mathcal{M} = -P\Lambda_\delta \sum_{n=0}^{+\infty} [-(I-P)\mathcal{U}^G \Lambda_\delta]^n \tag{32}$$

An exact solution of the Dyson equation cannot be obtained due to the infinite sum in the expression for the mass operator and an approximate solution is derived.

### 4.2 *The Foldy approximation*

In the following, the Foldy approximation is applied to estimate the configurationally averaged field by means of the solution in the single scatterer case. The Foldy approximation [11] is a mean field approximation for the wavefield $\mathbf{u}'_{\mathrm{i}j}$ incident on building $j$. This wavefield is composed of the wavefields $\mathbf{u}'_{\mathrm{d}k}$ scattered by all other buildings:

$$\mathbf{u}'_{\mathrm{i}j} = \mathbf{u}_\mathrm{i} + \sum_{k=1, k\neq j}^{N} \mathbf{u}'_{\mathrm{d}k} \tag{33}$$

The scattering operator $\mathcal{T}_k$ of a single building in equation (22) is now used to calculate the wavefield $\mathbf{u}'_{\mathrm{d}k}$, scattered by building $k$ from the incident field on building $k$:

$$\mathbf{u}'_{\mathrm{d}k} = \mathcal{U}^G \mathcal{T}_k \mathbf{u}'_{\mathrm{i}k} \tag{34}$$

This leads to the following system of $N$ equations and $N$ unknown for the exciting wavefields $\mathbf{u}'_{\mathrm{i}j}$:

$$\mathbf{u}'_{\mathrm{i}j} = \mathbf{u}_\mathrm{i} + \mathcal{U}^G \sum_{k=1, k\neq j}^{N} \mathcal{T}_k \mathbf{u}'_{\mathrm{i}k} \tag{35}$$

In a similar way as the Dyson equation has been derived from equation (13), an equation for the mean exciting wavefield can be formulated.

A first order approximation yields the following equation:

$$\underline{\mathbf{u}}'_\mathrm{i} = \mathbf{u}_\mathrm{i} + \mathcal{U}^G P \sum_{j=1}^{N} \mathcal{T}_j \underline{\mathbf{u}}'_\mathrm{i} \tag{36}$$

which is similar to the Foldy approximation [11] for the mean exciting field [12, 25] in the case of point scatterers. The averaging operation involves both a spatial averaging over all possible positions of the buildings and an averaging over the building impedance $i\omega\mathbf{Z}'_j$:

$$\underline{\mathbf{u}}(\mathbf{x}) = \mathbf{u}_\mathrm{i}(\mathbf{x}) - \rho_{sc} \int_S \mathbf{U}^G(\mathbf{x}, \mathbf{x}') \int_S \mathbf{\Pi}(\mathbf{x}' - \mathbf{x}_j) i\omega \underline{\mathbf{Z}}' \underline{\mathbf{u}}(\mathbf{x}_j)\, d\mathbf{x}_j\, d\mathbf{x}' \tag{37}$$

where $i\omega\underline{\mathbf{Z}}'$ denotes the mean modified building impedance and the mean exciting field is considered as an approximation of the mean field in the soil domain.

In the case of a horizontally layered half-space, this equation can be solved explicitly by means of a double forward Fourier transformation from the horizontal coordinates to the wavenumber pair $\mathbf{k}$. In the following, a distinction is therefore made between the horizontal coordinates $\mathbf{x}_S$ and the vertical coordinate $z$. The displacement field $\mathbf{u}(\mathbf{x})$ is rewritten as $\mathbf{u}(\mathbf{x}_S, z)$. Furthermore, in the case of a horizontally layered half-space, the Green's tensor is invariant under a horizontal translation and is rewritten as $\mathbf{U}^G(\mathbf{x}'_S - \mathbf{x}_S, z', z)$. The Foldy equation for the mean field now becomes:

$$\underline{\tilde{\mathbf{u}}}(\mathbf{k}, z) = \tilde{\mathbf{u}}_\mathrm{i}(\mathbf{k}, z) - \rho_{sc} \tilde{\mathbf{U}}^G(-\mathbf{k}, 0, z) \tilde{\mathbf{\Pi}}(\mathbf{k}) i\omega \underline{\mathbf{Z}}' \underline{\tilde{\mathbf{u}}}(\mathbf{k}, 0) \tag{38}$$

where a tilde denotes the wavenumber domain transform. The evaluation of this equation for $z = 0$ provides a system of three equations with three unknown $\underline{\tilde{\mathbf{u}}}(\mathbf{k}, 0)$ in the frequency–wavenumber domain:

$$\left\{\mathbf{I} + \rho_{sc}\tilde{\mathbf{U}}^G(-\mathbf{k}, 0, 0)\tilde{\mathbf{\Pi}}(\mathbf{k})i\omega\underline{\mathbf{Z}}'\right\}\underline{\tilde{\mathbf{u}}}(\mathbf{k}, 0) = \tilde{\mathbf{u}}_{\mathrm{i}}(\mathbf{k}, 0) \tag{39}$$

The solution of this equation gives the mean field $\underline{\tilde{\mathbf{u}}}(\mathbf{k}, 0)$ at the soil's surface, which can subsequently be used for the evaluation of the mean field at any depth $z$.

### 4.3 *The mean Green's function*

The Foldy approximation in equation (38) allows us to formulate the following equation for the mean Green's function of the coupled city-half-space system:

$$\underline{\tilde{U}}^G_{kn}(\mathbf{k}, z, z') = \tilde{U}^G_{kn}(\mathbf{k}, z, z') - \rho_{sc}\tilde{U}^G_{kl}(-\mathbf{k}, 0, z)\tilde{\Pi}_{lm}(\mathbf{k})i\omega\underline{Z}'_{mm}\underline{\tilde{U}}^G_{mn}(\mathbf{k}, 0, z') \tag{40}$$

where a summation on the dummy indexes $l$ and $m$ is performed. The calculation of the mean Green's tensor $\underline{\mathbf{U}}^G$ therefore requires the solution of a system of equations in terms of the Green's tensor $\underline{\tilde{U}}^G_{kn}(\mathbf{k}, 0, z')$ for the fundamental response at the soil's surface ($z = 0$).

In the following, the mean Green's functions are needed for the case where both the source and the receiver are located at the soil's surface ($z' = 0, z = 0$) and the source and receiver directions are equal to $\mathbf{e}_x$ and $\mathbf{e}_y$. The equations for the Green's functions $\underline{\tilde{U}}^G_{xx}(\mathbf{k}, 0, 0)$, $\underline{\tilde{U}}^G_{yx}(\mathbf{k}, 0, 0)$ and $\underline{\tilde{U}}^G_{xy}(\mathbf{k}, 0, 0)$, $\underline{\tilde{U}}^G_{yy}(\mathbf{k}, 0, 0)$, respectively, uncouple as follows:

$$\begin{bmatrix} 1 + \rho_{sc}\tilde{U}^G_{xx}i\omega\underline{Z}'\tilde{\Pi} & \rho_{sc}\tilde{U}^G_{xy}i\omega\underline{Z}'\tilde{\Pi} \\ \rho_{sc}\tilde{U}^G_{yx}i\omega\underline{Z}'\tilde{\Pi} & 1 + \rho_{sc}\tilde{U}^G_{yy}i\omega\underline{Z}'\tilde{\Pi} \end{bmatrix} \begin{Bmatrix} \underline{\tilde{U}}^G_{xx} \\ \underline{\tilde{U}}^G_{yx} \end{Bmatrix} = \begin{Bmatrix} \tilde{U}^G_{xx} \\ \tilde{U}^G_{yx} \end{Bmatrix} \tag{41}$$

$$\begin{bmatrix} 1 + \rho_{sc}\tilde{U}^G_{xx}i\omega\underline{Z}'\tilde{\Pi} & \rho_{sc}\tilde{U}^G_{xy}i\omega\underline{Z}'\tilde{\Pi} \\ \rho_{sc}\tilde{U}^G_{yx}i\omega\underline{Z}'\tilde{\Pi} & 1 + \rho_{sc}\tilde{U}^G_{yy}i\omega\underline{Z}'\tilde{\Pi} \end{bmatrix} \begin{Bmatrix} \underline{\tilde{U}}^G_{xy} \\ \underline{\tilde{U}}^G_{yy} \end{Bmatrix} = \begin{Bmatrix} \tilde{U}^G_{xy} \\ \tilde{U}^G_{yy} \end{Bmatrix} \tag{42}$$

where the dependence of the Green's functions on the wavenumber $\mathbf{k}$ and the coordinates $z = z' = 0$ is omitted. A change of coordinates from the wavenumber pair $\mathbf{k}$ to a radial wavenumber $k_r$ and an angular coordinate $\theta$ is performed to calculate the Green's functions of the original elastic half-space from the results of a reflection-transmission method [26] that have been obtained by means of a Hankel transform in a cylindrical coordinate system. The mean Green's functions show the same angular dependence on $\theta$ as the original Green's functions, as expected from the configurational averaging over the disorder.

In the following, the attenuation of the mean and the original Green's function are compared to verify the simplified estimation of the mean free path in equation (29).

## 5. The field correlation

### 5.1 *The Bethe–Salpeter equation*

The Bethe–Salpeter equation [14] is an equation on the configurationally averaged outer product of the wavefield $\mathbf{u}(\mathbf{x}, t)$ or its correlation function $\mathbf{R}(\mathbf{x}, \mathbf{x}', t, t')$. The power spectrum $\mathbf{S}(\mathbf{x}, \mathbf{x}', \omega, \omega')$ is the double Fourier transform of the correlation function with respect to $t$ and $t'$:

$$\mathbf{S}(\mathbf{x}, \mathbf{x}', \omega, \omega') = \boldsymbol{E}[\mathbf{u}(\mathbf{x}, \omega) \otimes \mathbf{u}^*(\mathbf{x}', \omega')] \tag{43}$$

The non-stationary Bethe–Salpeter equation for the field correlation is formulated as follows [14, 16]:

$$\mathbf{S}(\mathbf{x}, \mathbf{x}', \omega, \omega') = \underline{\mathbf{u}}(\mathbf{x}, \omega) \otimes \underline{\mathbf{u}}^*(\mathbf{x}', \omega') + \int_D \int_D \int_D \int_D \underline{\mathbf{U}}^G(\mathbf{x}', \mathbf{y}'_1, \omega) \otimes \underline{\mathbf{U}}^{G*}(\mathbf{x}'', \mathbf{y}''_1, \omega') : \\ \times \mathbf{K}(\mathbf{y}'_1, \mathbf{y}''_1, \mathbf{x}'_1, \mathbf{x}''_1, \omega, \omega') : \mathbf{S}(\mathbf{x}'_1, \mathbf{x}''_1, \omega, \omega')\, d\mathbf{y}'_1\, d\mathbf{y}''_1\, d\mathbf{x}'_1\, d\mathbf{x}''_1 \tag{44}$$

where $\mathbf{K}(\mathbf{y}'_1, \mathbf{y}''_1, \mathbf{x}'_1, \mathbf{x}''_1, \omega, \omega')$ represents the kernel of the intensity operator, which is expressed as an infinite sum of operators by means of a diagram approach [14, 16]. In order to avoid a laborious notation, the dependence on $\omega$ and $\omega'$ is omitted and understood implicitly. The solution of the Bethe–Salpeter equation allows us to calculate the configurationally averaged non-stationary field correlation.

### 5.2 *The ladder approximation*

In the ladder approximation, the infinite sum that determines the kernel of the intensity operator is truncated at its first term. This leads to the following expression for the intensity operator that is based on the solution of the single scatterer problem:

$$\mathbf{K}(\mathbf{y}'_1, \mathbf{y}''_1, \mathbf{x}'_1, \mathbf{x}''_1) = \rho_{sc} \int_S \langle \mathbf{\Pi}(\mathbf{y}'_1 - \mathbf{x}_\mathrm{b}) i\omega \mathbf{Z}'_j \otimes \mathbf{\Pi}^*(\mathbf{y}'_1 - \mathbf{x}_\mathrm{b})(i\omega' \mathbf{Z}'_j)^* \rangle \\ \times \delta(\mathbf{y}'_1 - \mathbf{x}'_1)\delta(\mathbf{y}''_1 - \mathbf{x}''_1)\, d\mathbf{x}_\mathrm{b} \tag{45}$$

In the present paper, independent approximating solutions of the Dyson and Bethe–Salpeter equation are made. The conservation of energy is therefore not demonstrated through the derivation of a Ward identity that links both approximations. The ladder approximation of the Bethe–Salpeter equation for the field correlation is:

$$\mathbf{S}(\mathbf{x}', \mathbf{x}'') = \underline{\mathbf{u}}(\mathbf{x}') \otimes \underline{\mathbf{u}}^*(\mathbf{x}'') + \rho_{sc} \int_S \int_S \int_S \underline{\mathbf{U}}^G(\mathbf{x}', \mathbf{x}'_1) \otimes \underline{\mathbf{U}}^{G*}(\mathbf{x}'', \mathbf{x}''_1) : \\ \times \langle \mathbf{\Pi}(\mathbf{x}'_1 - \mathbf{x}_\mathrm{b}) i\omega \mathbf{Z}_j \otimes \mathbf{\Pi}^*(\mathbf{x}''_1 - \mathbf{x}_\mathrm{b}) \times (i\omega' \mathbf{Z}'_j)^* \rangle : \mathbf{S}(\mathbf{x}'_1, \mathbf{x}''_1)\, d\mathbf{x}'_1\, d\mathbf{x}''_1\, d\mathbf{x}_\mathrm{b} \tag{46}$$

In the case of a field that is second moment stationary with respect to the horizontal position, $\mathbf{S}(\mathbf{x}', \mathbf{x}'')$ can be rewritten as $\mathbf{S}(\mathbf{x}''_S - \mathbf{x}'_S, z'', z')$. The mean Green's tensor $\underline{\mathbf{U}}^G(\mathbf{x}', \mathbf{x})$ of a horizontally layered half-space is invariant under a horizontal translation and can be replaced by $\underline{\mathbf{U}}^G(\mathbf{x}_S - \mathbf{x}'_S, z, z')$. In a similar way as in the mean field approximation, the solution of the correlation at the soil's surface ($z = 0, z' = 0$) will allow for the calculation of any other pair $(z, z')$. In the following, the vertical coordinates are therefore omitted and it is assumed implicitly that all functions are evaluated at $z = 0$ and $z' = 0$, leading to the following expression for the field correlation at the soil's surface:

$$\mathbf{S}(\mathbf{x}''_S - \mathbf{x}'_S) = \underline{\mathbf{u}}(\mathbf{x}'_S) \otimes \underline{\mathbf{u}}^*(\mathbf{x}''_S) + \rho_{sc} \int_S \int_S \int_S \underline{\mathbf{U}}^G(\mathbf{x}'_{1S} - \mathbf{x}'_S) \otimes \underline{\mathbf{U}}^{G*}(\mathbf{x}''_{1S} - \mathbf{x}''_S) : \\ \times \langle \mathbf{\Pi}(\mathbf{x}'_{1S} - \mathbf{x}_{\mathrm{b}S}) i\omega \mathbf{Z}'_j \otimes \mathbf{\Pi}^*(\mathbf{x}''_{1S} - \mathbf{x}_{\mathrm{b}S})(i\omega' \mathbf{Z}'_j)^* \rangle : \\ \times \mathbf{S}(\mathbf{x}''_{1S} - \mathbf{x}'_{1S})\, d\mathbf{x}'_{1S}\, d\mathbf{x}''_{1S}\, d\mathbf{x}_{\mathrm{b}S} \tag{47}$$

The two terms containing the distribution of tractions $\mathbf{\Pi}$ vanish when either $\mathbf{x}'_1$ or $\mathbf{x}''_1$ are not on the interface $\Gamma_j$ of a building located at $\mathbf{x}_\mathrm{b}$. If we assume that the field correlation varies on a scale that is larger than the scale of an individual foundation, $\mathbf{S}(\mathbf{x}''_{1S} - \mathbf{x}'_{1S})$ can be approximated by $\mathbf{S}(0)$. In the frequency–wavenumber domain, the following expression is

obtained:

$$\tilde{\mathbf{S}}(\mathbf{k}) = \int_S \underline{\mathbf{u}}(\mathbf{x}'_S) \otimes \underline{\mathbf{u}}^*(\mathbf{x}''_S) \exp\left[+i\mathbf{k}(\mathbf{x}''_S - \mathbf{x}'_S)\right] d\mathbf{x}''_S + \rho_{sc} \underline{\tilde{\mathbf{U}}}^G(\mathbf{k}) \otimes \underline{\tilde{\mathbf{U}}}^{G*}(\mathbf{k}):$$
$$\times \langle \tilde{\mathbf{\Pi}}(-\mathbf{k}) i\omega \mathbf{Z}'_j \otimes \tilde{\mathbf{\Pi}}^*(-\mathbf{k})(i\omega' \mathbf{Z}'_j)^* \rangle (:)\, \mathbf{S}(0) \tag{48}$$

This equation for $\tilde{\mathbf{S}}(\mathbf{k})$ is transformed into a system of equations on $\mathbf{S}(0)$, by means of an integration on all wavenumbers $\mathbf{k}$ and accounting for the identity:

$$\mathbf{S}(0) = \frac{1}{4\pi^2} \int \tilde{\mathbf{S}}(\mathbf{k})\, d\mathbf{k} \tag{49}$$

The following system of equations is finally obtained:

$$\mathbf{S}(0) = \underline{\mathbf{u}}(\mathbf{x}'_S) \otimes \underline{\mathbf{u}}^*(\mathbf{x}'_S) + \rho_{sc} \frac{1}{4\pi^2} \int \underline{\tilde{\mathbf{U}}}^G(\mathbf{k}) \otimes \underline{\tilde{\mathbf{U}}}^{G*}(\mathbf{k}):$$
$$\langle \tilde{\mathbf{\Pi}}(-\mathbf{k}) i\omega \mathbf{Z}'_j \otimes \tilde{\mathbf{\Pi}}^*(-\mathbf{k})(i\omega' \mathbf{Z}'_j)^* \rangle : \mathbf{S}(0)\, d\mathbf{k} \tag{50}$$

The solution for $\mathbf{S}(0)$ allows us to calculate the field correlation for any other wavenumber pair $\mathbf{k}$ by means of equation (48). In an indicial notation, each equation is written as:

$$S_{kl}(0) = \underline{u}_k(\mathbf{x}'_S) \underline{u}^*_l(\mathbf{x}'_S) + \rho_{sc} \langle i\omega Z'_{jmm} (i\omega' Z'_{jnn})^* \rangle$$
$$\times \left[ \frac{1}{4\pi^2} \int \underline{\tilde{U}}^G_{km}(\mathbf{k}) \tilde{\Pi}_{mm}(-\mathbf{k}) \underline{\tilde{U}}^{G*}_{ln}(\mathbf{k}) \tilde{\Pi}^*_{nn}(-\mathbf{k})\, d\mathbf{k} \right] S_{mn}(0) \tag{51}$$

where it has been assumed that $\tilde{\mathbf{\Pi}}(-\mathbf{k})$ is a diagonal matrix, as is the case for relaxed boundary conditions at the building–soil interface. Furthermore, as only the horizontal motion of the buildings will be considered, $k, l, m$ and $n$ only refer to $x$ or $y$. The integral inside the square brackets in equation (51) is denoted as $\phi_{klmn}$ and depends on the circular frequencies $\omega$ and $\omega'$ only:

$$\phi_{klmn} = \frac{1}{4\pi^2} \int \underline{\tilde{U}}^G_{km}(\mathbf{k}) \underline{\tilde{U}}^{G*}_{ln}(\mathbf{k}) \tilde{\Pi}_{mm}(-\mathbf{k}) \tilde{\Pi}^*_{nn}(-\mathbf{k})\, d\mathbf{k} \tag{52}$$

This integral is solved by means of a change of variables from $\mathbf{k}$ to the radial wavenumber $k_r$ and an angular coordinate $\theta$. In the case where the foundation shape is circular and the stress distribution $\tilde{\Pi}$ is uniform in both directions, the integrand depends on $\theta$ through the mean Green's functions only. This angular dependence uncouples the equations for $S_{xy}(0)$ and $S_{yx}(0)$ from those for $S_{xx}(0)$ and $S_{yy}(0)$.

## 6. The response of a city to a vertically incident shear wave

### 6.1 *The Roma Norte district of Mexico City*

In the following, the configurationally averaged site response and correlation are calculated for the case of the Roma Norte district of Mexico City, subjected to a plane, vertically incident shear wave (SH wave). This is the most relevant case in earthquake engineering since, due to the velocity contrast between the deeper and surface layers, almost all incident rays from the seismic source are converted into vertical rays, as stated by the Snell-Descartes law. For some particular sites such as the lake region in Mexico City, the waves diffracted by the edge of the basin can reach a significant amplitude, but still less than the direct wavefield.

The results are validated by means of numerical results of Mezher et al. [6] for a three-dimensional model of an entire city quarter. This model includes 77 buildings on a total surface

of $350 \times 450$ m$^2$. The buildings are modelled by means of the finite element method (FEM), using beam and plate elements for the beams and columns and the floors of the buildings, respectively. The buildings are coupled to the soil by means of the boundary element method (BEM), based on the Green's functions of the horizontally layered half-space. This allows us to fully account for the multiple wave scattering between the buildings. Assuming ergodicity, the spatial average of the site response and the correlation for this particular city configuration can be compared to the configurationally averaged quantities obtained within the present analysis.

### 6.2 *The soil model*

The soil is modelled as a horizontally layered linear elastic half-space for which the Green's functions [27, 28] are calculated numerically in the wavenumber–frequency domain by means of a reflection-transmission method [26].

Table 1 summarizes the layer thickness $t$, the shear wave velocity $C_s$, the longitudinal wave velocity $C_p$, the density $\rho$ and the material damping ratio $\beta$ of the soil model for the Mexico City lake bed zone. Material damping in the soil is modelled in the frequency domain by the use of complex Lamé coefficients $\lambda(1+2\beta i)$ and $\mu(1+2\beta i)$, where $\beta$ represents the hysteretic material damping ratio. The interface between layer 14 and the half-space 15 is referred to as the bedrock level in the following.

In the case of a vertically incident SH wave in a horizontally layered half-space, the total wavefield in the soil layers consists of upward and downward vertically propagating waves and can be formally written as $u_x[\exp(+ik_\alpha z) + \exp(-ik_\alpha z)]\mathbf{e}_x$ or $u_x(z)\mathbf{e}_x$. The site transfer function relates, in the frequency domain, the site response $u_x(0)$ at the soil's surface ($z = 0$) to the incident, upward propagating SH wave $u_{\mathrm{ix}}(z_{\mathrm{br}})$ at bedrock level ($z = z_{\mathrm{br}}$). The dynamic soil characteristics in table 1 have been used to calculate the site transfer function in absence of the city. The transfer function (figure 2) shows a strong amplification with a factor of 20 near 0.4 Hz. This well-known amplification of the ground motion is also found when data recorded at the lake bed zone of Mexico City are compared to data from hill zones [2] and is attributed to the first site resonance frequency. This first site resonance is due to the presence of a highly compressible clay with a shear wave velocity of about 70 m/s in the upper 30 to 80 m of soil. A second site resonance frequency is observed near 0.8 Hz.

Table 1. The dynamic soil characteristics.

| Layer | $t$ [m] | $C_s$ [m/s] | $C_p$ [m/s] | $\rho$ [kg/m$^3$] | $\beta$ [−] |
|---|---|---|---|---|---|
| 1 | 5 | 91 | 1447 | 1200 | 0.02 |
| 2 | 8 | 30 | 1447 | 1100 | 0.02 |
| 3 | 14 | 55 | 1233 | 1100 | 0.02 |
| 4 | 8 | 80 | 1267 | 1200 | 0.02 |
| 5 | 8 | 202 | 1442 | 1400 | 0.02 |
| 6 | 8 | 131 | 1472 | 1400 | 0.02 |
| 7 | 5 | 404 | 1786 | 1500 | 0.01 |
| 8 | 10 | 253 | 1588 | 1500 | 0.01 |
| 9 | 38 | 434 | 1746 | 1700 | 0.01 |
| 10 | 20 | 666 | 1965 | 1700 | 0.01 |
| 11 | 8 | 434 | 1771 | 1700 | 0.01 |
| 12 | 10 | 929 | 1935 | 1900 | 0.01 |
| 13 | 22 | 505 | 1776 | 1800 | 0.01 |
| 14 | 14 | 677 | 2084 | 1800 | 0.01 |
| 15 | $\infty$ | 1132 | 2522 | 2000 | 0.01 |

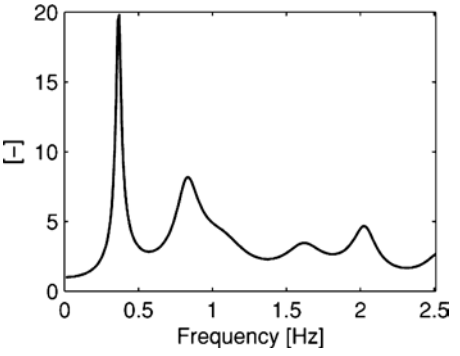


Figure 2. Site transfer function.

The incident wavefield $\mathbf{u}_{\mathrm{i}}(\mathbf{x}, t)$ in the following is the total wavefield in the soil generated by an incident wave $u_{\mathrm{ix}}(z_{\mathrm{br}}, t) = f(t)$, where $f(t)$ is a Ricker pulse, centred at 0.75 Hz in the frequency domain (figure 3). Figure 4a shows the frequency content of this incident wavefield $u_{\mathrm{ix}}(0)$ at the soil's surface, which is obtained as the product of the site transfer function in figure 2 and the frequency content $f(\omega)$ of the incoming wave at bedrock level. The time history in figure 4b is obtained by means of an inverse Fourier transform and clearly shows the contribution of the first site resonance. Due to the velocity contrast between the upper soil layers and the underlying half-space (table 1), the downward propagating waves are almost perfectly reflected and the attenuation observed in figure 4b is mainly due to absorption in the soil.

### 6.3 *The city model*

The statistical model of the dynamic characteristics of the buildings is based on the distribution of the number of storeys over all buildings in the city. Figure 5a shows the built surface as a function of the number of storeys $n$ for the city quarter. The fundamental resonance frequency of the buildings is estimated as $10/n$, which leads to the distribution of the horizontal building resonance frequency shown in figure 5b. The same resonance frequency is considered for the motion in the $x$- and $y$-direction. It is important to notice that these resonance frequencies are well above the first site resonance frequency at 0.4 Hz, as observed in the site transfer function (figure 2). All buildings are assumed to have the same foundation surface $S_b = 625\,\mathrm{m}^2$ and a damping ratio $\zeta$ of 0.05. The building mass $m$ is estimated from the number of floors $n$ and the foundation size $S_b$ as $0.36 n \rho_b S_b$, where $\rho_b$ has a value of $2500\,\mathrm{kg/m}^3$, corresponding to

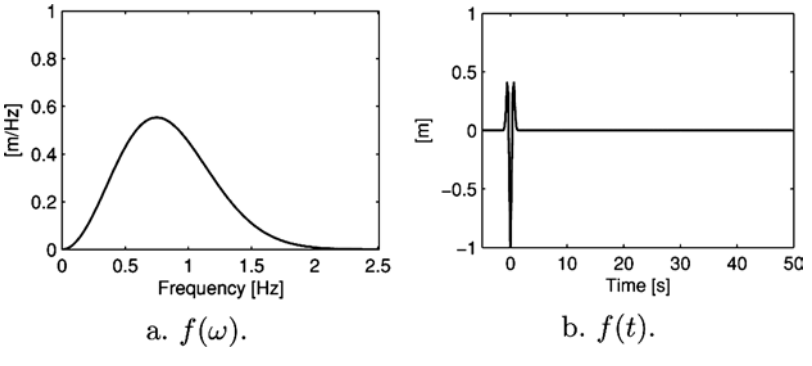


Figure 3. (a) Frequency content and (b) time history of the incident wave $u_{\mathrm{ix}}(z_{\mathrm{br}}, t) = f(t)$.

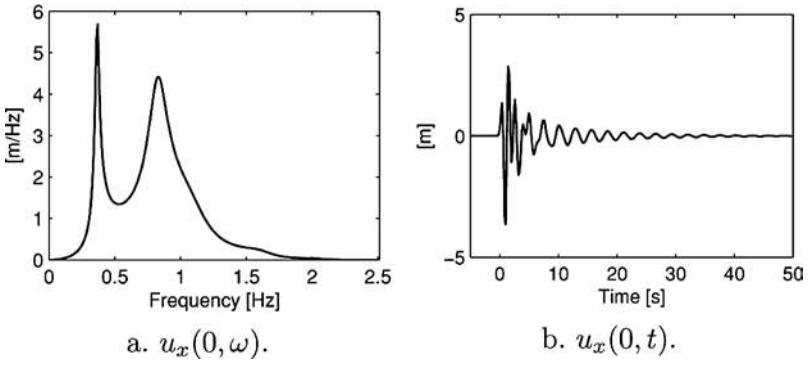


Figure 4. (a) Frequency content and (b) time history of the incident wavefield $u_{ix}(0)$ at the soil's surface.

reinforced concrete and 0.36 m is an equivalent floor slab thickness that allows us to obtain similar masses as in the deterministic city model.

The surface density $\rho_{sc}$ of the buildings is calculated from the foundation size $S_b = 625\,\mathrm{m}^2$ and the ratio $\eta = 0.32$ of the built surface and the total surface as $\eta/S_b$, resulting in a value of $5.1 \times 10^{-4}\,\mathrm{m}^{-2}$.

Figure 6 shows the impedance $i\omega Z$ for a building with 10 floors, as calculated from equation (7), with an estimated resonance frequency of 1 Hz. The building mass in this equation has been corrected for the fact that only 81% of the mass participates in the first horizontal mode, which leads to an additional term of $-0.19\ \mathrm{m}\omega^2$ for the impedance. At frequencies $\omega$ low compared to the resonance frequency $\omega_{\mathrm{res}}$, the building impedance is dominated by the inertial term. At the resonance frequency, the real part of the impedance vanishes and the imaginary part reaches a maximum. At high frequencies, the real part tends to a value of $-0.19\ \mathrm{m}\omega^2$.

### 6.4 *The single scatterer problem*

The computation of the mean field by means of the Foldy equation requires the solution of the soil-structure interaction problem for a single building. Equation (22) shows how this solution is obtained by the calculation of the modified building impedance $i\omega Z'$ that corresponds to a series connection of the soil impedance $K_s$ and the impedance $i\omega Z$.

The boundary element method (BEM) [29], based on the Green's functions of the soil model in table 1, has been used to calculate the soil impedance $K_s$ (figure 7a). The imaginary

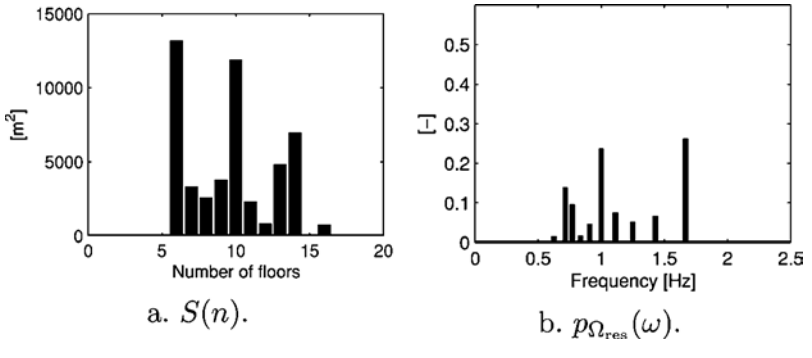


Figure 5. (a) Built surface $S$ as a function of the number $n$ of floors and (b) distribution of the building resonance frequency $\Omega_{\mathrm{res}}$.

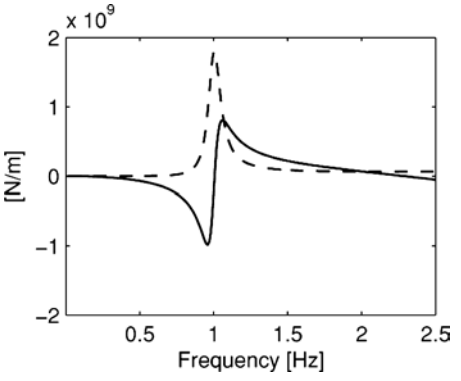


Figure 6. Real (solid line) and imaginary (dashed line) part of the building impedance $i\omega Z$ for a building with 10 floors.

part of the soil impedance represents the energy dissipation due to the radiation of waves and absorption in the soil. Figure 7b shows the modified impedance $i\omega Z'$ for a building with 10 floors. At frequencies low compared to the resonance frequency, the impedance $i\omega Z$ has a negative value and the building acts as an additional mass at the soil's surface. At the resonance frequency, the imaginary part reaches a maximum and the effect of multiple wave scattering will be the most pronounced.

A comparison of the impedance $i\omega Z$ in figure 6 and the modified impedance $i\omega Z'$ clearly illustrates the effects of soil–structure interaction for a single building. First, the additional soil flexibility lowers the fundamental building resonance frequency. Second, the coupling with the soil provides an additional damping mechanism through radiation and material damping in the soil.

Based on the results for the deterministic building impedances, the mean building impedance is calculated (figure 8). The results at low and high frequencies are similar to those for a particular building. In the frequency range of the building resonance frequencies, the imaginary part shows a uniform large value.

### 6.5 *The mean field*

In order to calculate the mean field approximation by means of equation (38), the representation of the incident wavefield in the frequency-wavenumber domain is calculated as:

$$\tilde{\mathbf{u}}_{\mathrm{i}}(\mathbf{k}, z) = 4\pi^2 \boldsymbol{\delta}(\mathbf{k}) u_{\mathrm{i}x}(z, \omega)\mathbf{e}_x \tag{53}$$

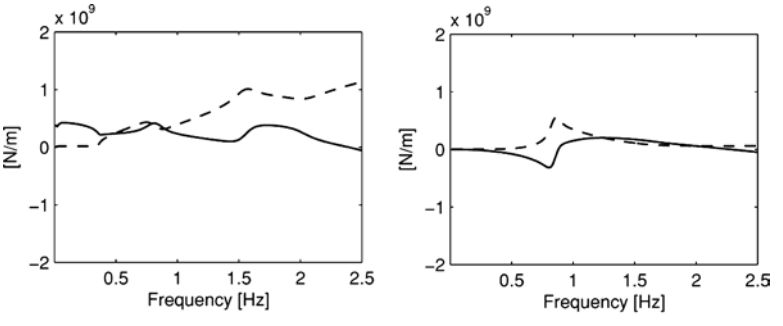


Figure 7. Real (solid line) and imaginary (dashed line) of (a) the soil impedance $K_s$ and (b) the modified impedance $i\omega Z'$.

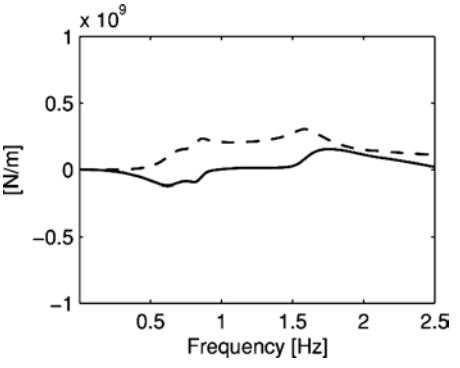


Figure 8. Real (solid line) and imaginary (dashed line) of the mean modified impedance $i\omega\underline{Z}'$.

The mean field necessarily has the same $\boldsymbol{\delta}(\mathbf{k})$ dependence on $\mathbf{k}$ and can be written as $4\pi^2\boldsymbol{\delta}(\mathbf{k})\underline{\mathbf{u}}(z)$. After a double inverse Fourier transformation from $\mathbf{k}$ to $\mathbf{x}_S$, the following system of equations is found for the mean field at the soil's surface:

$$[\mathbf{I} + \rho_{sc}\tilde{\mathbf{U}}^G(-\mathbf{k} = 0, 0, 0)i\omega\underline{\mathbf{Z}}'\tilde{\boldsymbol{\Pi}}(\mathbf{k} = 0)]\ \underline{\mathbf{u}}(0) = \mathbf{u}_{\mathrm{i}}(0) \tag{54}$$

The mean field $\underline{\mathbf{u}}(z)$ at an arbitrary depth $z$ is calculated from the mean field $\underline{\mathbf{u}}(0)$ at the soil's surface by means of equation (38). The matrix $\tilde{\boldsymbol{\Pi}}(\mathbf{k} = 0)$ in equation (54) equals the unity matrix $\mathbf{I}$ as an evaluation of a function at a wavenumber $\mathbf{k} = 0$ is equivalent to an integration in the spatial domain over all $\mathbf{x}$. Furthermore, the equations for the displacement components of $\underline{\mathbf{u}}$ decouple due to the fact that the Green's tensor $\tilde{\mathbf{U}}^G(-\mathbf{k} = 0, 0, 0)$, the modified impedance $i\omega\mathbf{Z}'$ and the traction distribution matrix $\tilde{\boldsymbol{\Pi}}(\mathbf{k} = 0)$ are diagonal matrices. The mean field is therefore zero in the directions $\mathbf{e}_y$ and $\mathbf{e}_z$ and only has a non-vanishing component $\underline{u}_x$.

Figure 9 shows the modulus of the ratio of the mean field $\underline{u}_x(0)$ and the incident wavefield $u_{\mathrm{i}x}(0)$ at the soil's surface. The ratio shows an increase at low frequencies until a peak is reached at approximately 0.32 Hz, that is followed by a steep descent with a minimum at 0.37 Hz and a slow rise to a value of approximately 1. The sharp peak at 0.32 Hz suggests an amplification of the incident field, but merely corresponds to a shift of the first site resonance frequency, as indicated by the steep descent to a value much lower than unity that follows it.

Figure 10 compares the frequency content of the original site response due to a vertically incident SH wave with the mean response as obtained by the Foldy approximation and the

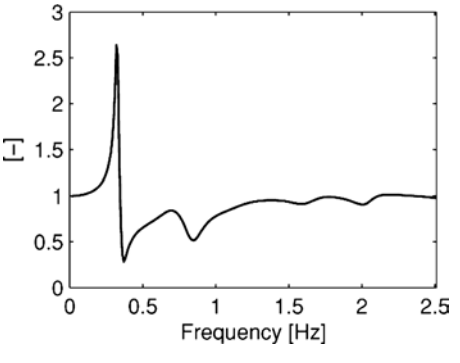


Figure 9. Modulus of the ratio of the mean field $\underline{u}_x(0)$ and the wavefield $u_{\mathrm{i}x}(0)$ at the soil's surface as obtained by the Foldy approximation.

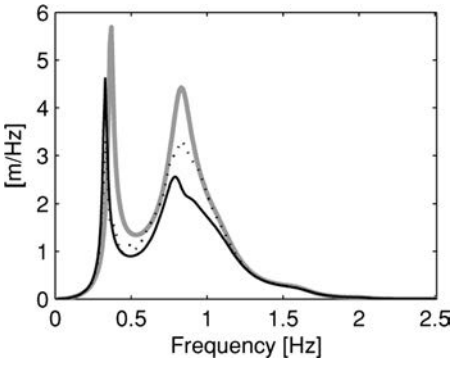


Figure 10. Frequency content of the response at the soil's surface due to a vertically incident SH wave for the original site (grey line) and frequency content of the mean response as obtained by the Foldy approximation (solid line) and the FEM-BEM calculation (dotted line).

spatial averaging of the results for the city of finite size in the FEM-BEM computation. Comparing the Foldy approximation to the original site transfer function, a clear shift of the first site resonance frequency is observed due to the inertial behaviour of the mean impedance in this frequency range (figure 8). The lower value for the mean transfer function near 0.8 Hz may be due to wave scattering and absorption by the buildings. In the case of the FEM-BEM calculations, the mean site transfer function has been computed from the mean field at the soil's surface in between the buildings. These results show a shift of the first site resonance frequency, as for the Foldy approximation, but with a slightly lower peak value. The decrease near 0.8 Hz is less pronounced and the response is closer to the original site transfer function.

Figure 11 compares the time history of the original site response due to a vertically incident SH wave with the mean response as obtained by the Foldy approximation and the FEM-BEM calculation. The modulus of the time history is shown with a logarithmic vertical scale, so that the decay of the different fields can be better appreciated. When the original site response and the Foldy mean response are compared, it is observed that the peak value of the mean field is slightly smaller. The period of oscillation of the mean response is larger, as expected from the shift of the first resonance frequency. Furthermore, the mean response decays slower than the original site response, although it is also affected by the wave scattering and the absorption by the buildings. The slower decay is explained by the shift of the first resonance frequency. If, due to absorption in the soil, the original site response decays as $\exp(-\zeta_{\text{site}}\omega_{\text{site}}t)$, a decrease of

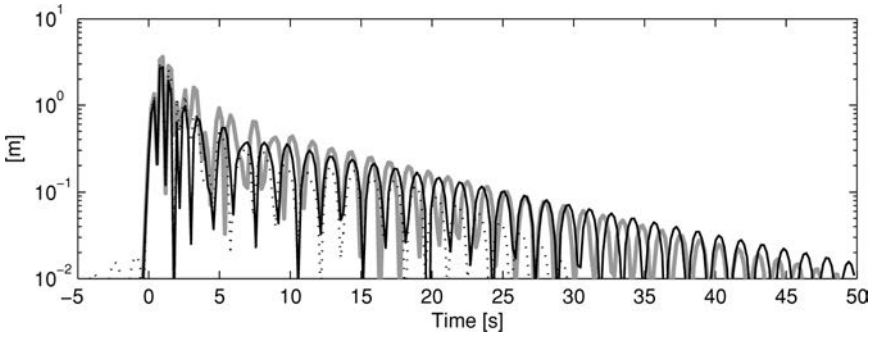


Figure 11. Time history of the response at the soil's surface due to a vertically incident SH wave for the original site (grey line) and time history of the mean response as obtained by the Foldy approximation (solid line) and the FEM-BEM calculation (dotted line).

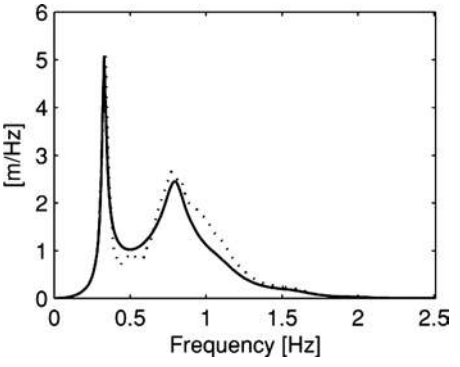


Figure 12. Frequency content of the mean foundation response as obtained by the Foldy approximation (solid line) and the FEM-BEM calculation (dotted line).

the site resonance frequency $\omega_{\text{site}}$ slows down the decay if the damping ratio $\zeta_{\text{site}}$ is unaffected. The results of the FEM-BEM calculation are close to the original site response at early times and show a larger oscillation period than the results by the Foldy approximation.

Equation (16) shows how the solution of the soil–structure interaction problem for a single building allows us to calculate the foundation response from the incident wavefield. This relation has been used to compute a mean transfer function that relates the foundation response to the incident wavefield. Figure 12 compares the mean foundation response, calculated as the product of the mean incident field and the mean transfer function with the results of the FEM-BEM calculation. A better agreement is found for the peak value of the response at the first site resonance frequency, as well as for the response in the range of the building resonance frequencies.

Figure 13 compares the mean foundation response in the time domain. A good agreement is found at small times, while at larger times between 5 s and 25 s, the Foldy approximation predicts a smaller mean response.

### 6.6 *The mean Green's function*

In order to verify the attenuation with distance of the response of the coupled city–soil system due to wave scattering and absorption by the buildings, the mean Green's function, $\underline{U}^G_{xx}(\mathbf{x}_S, z, z')$ is calculated from the solution of the system of equations (40) and compared to the Green's function of the original site.

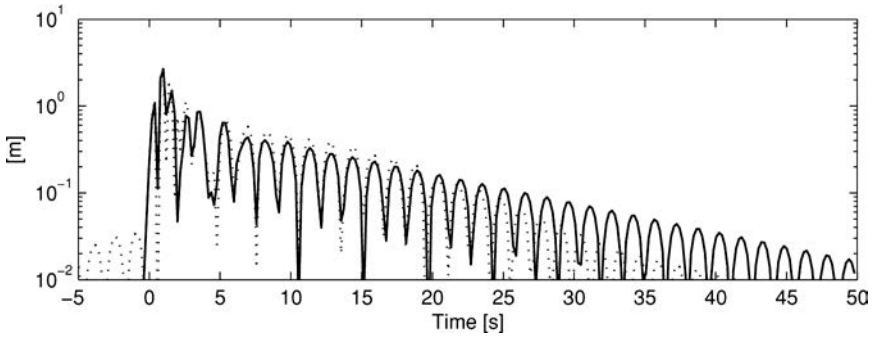


Figure 13. Time history of the mean foundation response as obtained by the Foldy approximation (solid line) and a FEM-BEM calculation (dotted line).

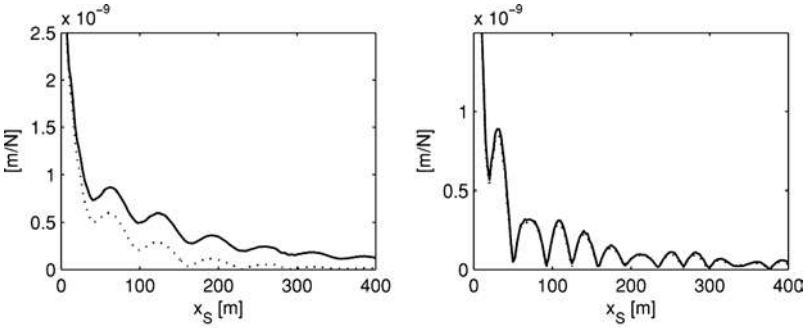


Figure 14. The Green's function $U^G_{xx}(x_S, y_S = 0, z = 0, z' = 0)$ of the layered half-space (solid line) and the mean Green's function $\underline{U}^G_{xx}(x_S, y_S = 0, z = 0, z' = 0)$ of the coupled city-half-space system (dotted line) at a frequency of (a) 1.0 Hz (b) 2.0 Hz.

Figure 14a compares the mean Green's function $\underline{U}^G_{xx}(x_S, y_S = 0, z = 0, z' = 0)$ of the coupled city-half-space system with the deterministic Green's function of the layered half-space as a function of $x_S$ at a frequency of 1 Hz. The mean Green's function is clearly more severely attenuated due to the combined effect of the wave scattering and the absorption by the buildings. The mean free path $l$ is estimated from the attenuation as 60 m and is of the same order of magnitude as the Rayleigh wavelength in the soil as indicated by the initial simplified estimation that only accounts for the attenuation due to wave scattering. Figure 14b shows similar results at a frequency of 2 Hz, which is beyond the range of resonance frequencies in figure 5b. The mean Green's function and the deterministic Green's now show a similar behaviour.

### 6.7 *Frequency content of the coherent and incoherent field*

In order to estimate the contribution of the waves scattered by the buildings to the total site response, the system of equations (51) that corresponds to the ladder approximation of the Bethe–Salpeter equation has been solved to calculate the field correlation $\mathbf{S}(\mathbf{x}''_S - \mathbf{x}'_S, z'', z', \omega, \omega')$, for the case where $\mathbf{x}''_S = \mathbf{x}'_S$ and $z'' = z' = 0$, denoted as $\mathbf{S}(0, \omega, \omega')$ in the following. For $\omega = \omega'$, this is the spatial average of the mean square modulus of the site response, which includes the contribution of the waves scattered by the buildings. The ratio of the mean square modulus $S_{xx}(0, \omega, \omega)$ and the square modulus $|\underline{u}_x|^2$ of the mean site response therefore indicates the importance of the scattered waves in the total site response.

Figure 15 shows the ratio of $S_{xx}(0, \omega, \omega)$ and $S_{yy}(0, \omega, \omega)$ and the square modulus $|\underline{u}_x|^2$ of the mean site response. At low frequencies, the ratio $S_{xx}(0, \omega, \omega)/|\underline{u}_x|^2$ is close to 1, while the mean square modulus of the response in the direction $\mathbf{e}_y$ is zero. In this frequency range, the total site response is equal to the mean site response. At higher frequencies between 0.4 Hz and 1.5 Hz, where the mean site response is lower than the original site response (figure 10), the ratio $S_{xx}(0, \omega, \omega)/|\underline{u}_x|^2$ is relatively large. This confirms the shift of the coherent site response to the incoherent component due to the scattering of waves by the buildings.

Figures 16a and b compare the mean square modulus of the seismic response at the soil's surface as obtained by the Foldy ladder approximation and the FEM-BEM calculation. Although the frequency content of the mean response in figure 10 is underestimated, a good agreement is found for the mean square modulus of the response in the direction $\mathbf{e}_x$. The main

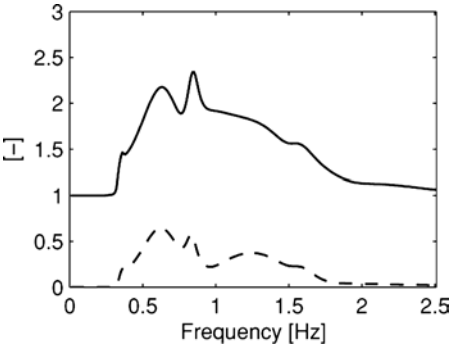


Figure 15. The ratio of the correlation $S_{xx}(0, \omega, \omega)$ (solid line), $S_{yy}(0, \omega, \omega)$ (dashed line) and the square modulus of the mean field $|\underline{u}_x|^2$.

difference between both results is therefore the way in which the total response is composed of the coherent and incoherent response. As the response in the direction $\mathbf{e}_y$ is entirely due to waves scattered by the buildings, the larger contribution of the scattered waves in the Foldy approximation also leads to a larger response.

### 6.8 *The correlation length of the scattered wavefield*

The results for the field correlation $\mathbf{S}(\mathbf{x}_S, \omega, \omega')$ at the soil's surface allow to estimate the correlation length $l_{xx}$ of the scattered wavefield. First, a correlation surface $A_{xx}$ is calculated as:

$$A_{xx} = \frac{\int_S [S_{xx}(\mathbf{x}_S, \omega, \omega) - \underline{u}_x(0)\underline{u}_x^*(\mathbf{x}_S)]\, d\mathbf{x}_S}{S_{xx}(0, \omega, \omega) - |\underline{u}_x(0)|^2} \tag{55}$$

The integral in the numerator can be calculated from the evaluation of the field correlation $\tilde{S}_{xx}(\mathbf{k}, \omega, \omega)$ at $\mathbf{k} = 0$. The latter is obtained by means of equation (48) as a function of $S_{xx}(0, \omega, \omega)$ and $S_{yy}(0, \omega, \omega)$:

$$\begin{aligned} &\int_S [S_{xx}(\mathbf{x}_S, \omega, \omega) - \underline{u}_x(0)\underline{u}_x^*(\mathbf{x})]\, d\mathbf{x}_S \\ &\quad = \rho_{sc}\langle|i\omega Z'|^2\rangle \left[\left|\underline{\tilde{U}}_{xx}^G(0)\right|^2 S_{xx}(0, \omega, \omega) + \left|\underline{\tilde{U}}_{xy}^G(0)\right|^2 S_{yy}(0, \omega, \omega)\right] \end{aligned} \tag{56}$$

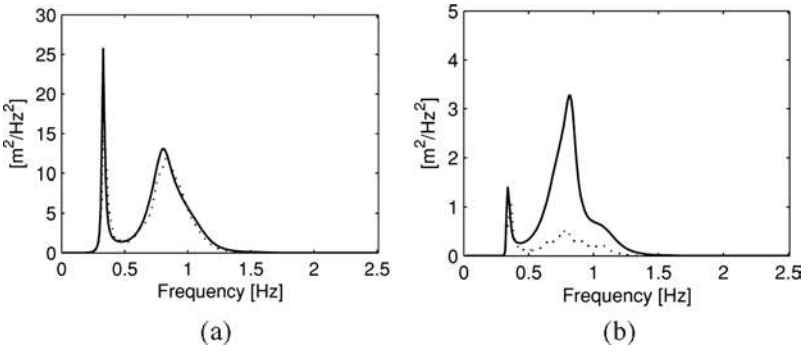


Figure 16. The correlation (a) $S_{xx}(0, \omega, \omega)$ and (b) $S_{yy}(0, \omega, \omega)$ of the exciting field as obtained by means of the Foldy ladder approximation (solid line) and a FEM-BEM calculation (dotted line).

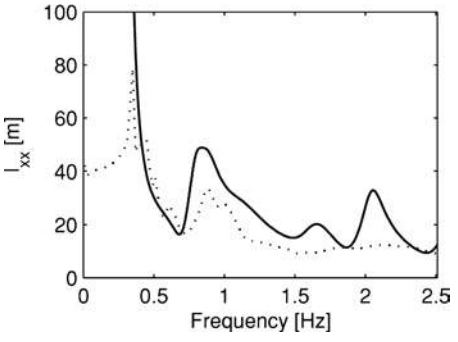


Figure 17. The correlation length of the incoherent field component as obtained by means of the Foldy ladder approximation (solid line) and the FEM-BEM calculation (dotted line).

where $|\tilde{\Pi}(0)|^2$ has been replaced by its unit value. The correlation length $l_{xx}$ is estimated from the correlation surface $A_{xx}$ as:

$$l_{xx} = 2\sqrt{\frac{A_{xx}}{\pi}} \tag{57}$$

Figure 17 compares the correlation length as computed by means of equations (55) and (57) with the correlation length of the wavefield in between the buildings from the FEM-BEM calculation. Both calculations show a correlation length that approximately decreases with the frequency as $1/\omega$. At low frequencies, the size of the city quarter in the deterministic model is small compared to the wavelength in the soil and the result is not valid. Although not visible on this figure, the correlation length as obtained from the approximate solution of the Bethe–Salpeter equation reaches a local maximum at the first site resonance frequency. Both calculations show a second local maximum at the second site resonance frequency of 0.8 Hz.

### 6.9 *Time history of the coherent and incoherent field*

The solution of the non-stationary Bethe–Salpeter equation in terms of $\mathbf{S}(0, \omega, \omega')$ allows us to recover the correlation function $\mathbf{R}(0, t, t')$ in the time domain by means of a double inverse Fourier transform from $\omega, \omega'$ to $t, t'$. An evaluation of the correlation function $\mathbf{R}(0, t, t')$ at $t = t'$ gives the mean square response in the time domain.

Figure 18 compares the time history of the square of the original site response with the mean square response as obtained by the Foldy ladder approximation and the FEM-BEM calculation. The peak value of the mean square response by the Foldy ladder approximation (figure 18a) is slightly smaller than the original site response. Whereas the original site response is attenuated due to absorption in the soil only, the attenuation of the mean square response is due to absorption in the soil and by the buildings. At larger times, however, the mean square response is found to be slightly larger than the original site response. The results of the FEM-BEM calculation in figure 18 are closer to the original site response, as expected due to the smaller contribution of scattered waves. As the mean square response is only slightly larger than the original site response, the presence of the city does not substantially increase the duration of the site response in the present case. For similar soil conditions, a clear increase of the signal duration has only been found in results of 2D models [8, 9], where relatively high buildings were considered with a resonance frequency close to the first site resonance frequency and a zero or low level of internal

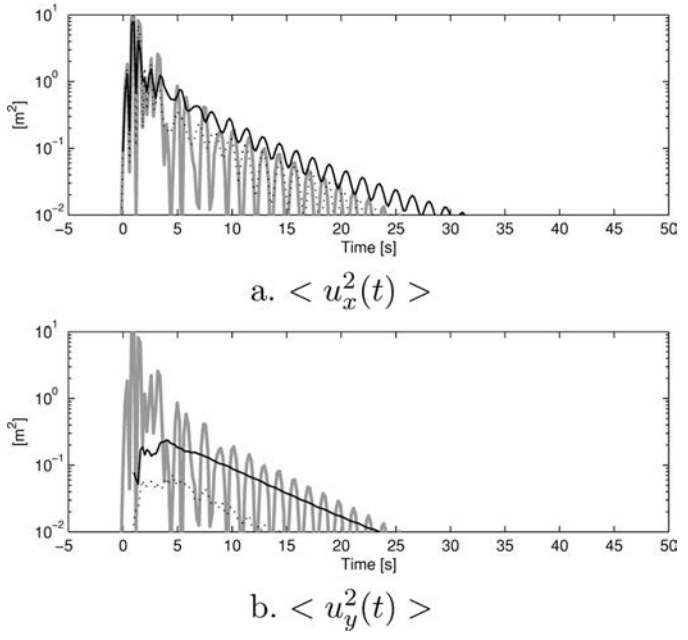


Figure 18. Time history of the square of the response at the soil's surface due to a vertically incident SH wave for the original site (grey line) and time history of the mean square response (a) $\langle u_x^2(t) \rangle$ and (b) $\langle u_y^2(t) \rangle$ as obtained by the Foldy ladder approximation (solid line) and the FEM-BEM calculation (dotted line).

damping. A more plausible explanation for the long duration of the seismic records in Mexico City is given by Shapiro et al. [30], who indicate that seismic records from the hill zone of the Mexico Valley and sites far from the urbanized area also show a long duration [30, 31].

The response in the direction $\mathbf{e}_y$ (figure 18b) only consists of the waves scattered by the buildings. Compared to the response in figure 18a, a time delay is observed. This is due to the fact that, after a building is excited by an incident wave, a certain time is required for the building to loose its energy by absorption and by radiation of waves into the soil. This results in a time delay for the incoherent field, which results from the scattered waves. If only radiation and absorption in the soil are accounted for, the dwell time $t_{\mathrm{dwell}} = 1/\omega_{\mathrm{ssi}}\zeta_{\mathrm{ssi}}$ determines the time scale on which energy is re-transmitted into the soil.

In order to investigate the role of the internal damping in the attenuation of the incoherent field, the results have been calculated for the case where the damping ratio $\zeta$ of the buildings equals zero. Figure 19 illustrates how the decay of the response in both horizontal directions changes drastically. In the direction $\mathbf{e}_x$, the attenuation changes in time due to the fact that the incoherent field builds up and attenuates more slowly than the coherent field. The attenuation of the incoherent field is directly observed in figure 19b that shows the response in the direction $\mathbf{e}_y$. The incoherent field attenuates more slowly than the mean field or original site response due to the fact that the buildings temporarily store energy after being excited, and energy is only lost during wave propagation by absorption in the soil. In this case, an increase of the duration of the response is observed. The same effect would slow down the transport of energy in the coupled city–soil system, as the time during which energy is stored adds up to the mean free propagation time between two buildings. These results show that resonant multiple wave scattering plays an important role in the seismic response of a city if the buildings do not absorb energy. The assumption of lossless scatterers

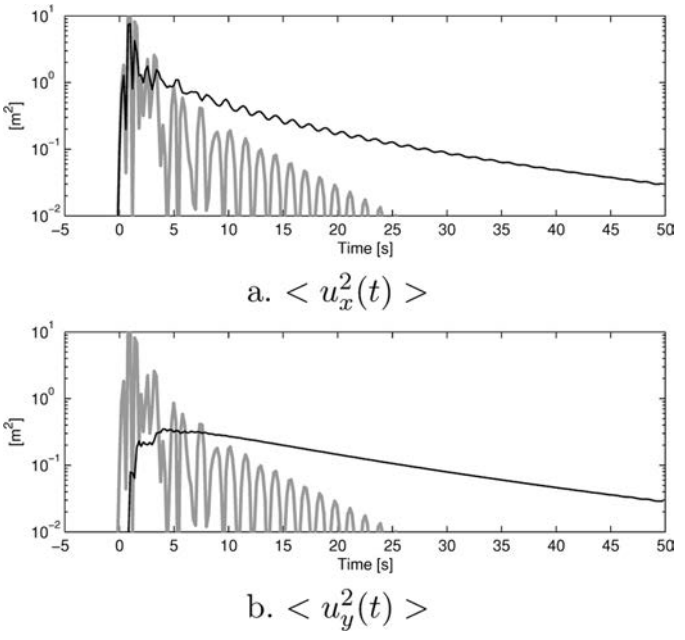


Figure 19. Time history of the square of the response at the soil's surface due to a vertically incident SH wave for the original site (grey line) and time history of the mean square response (a) $\langle u_x^2(t)\rangle$ and (b) $\langle u_y^2(t)\rangle$ as obtained by the Foldy ladder approximation (solid line) for the case where the damping ratio $\zeta$ of the buildings equals zero.

is not justified, however, when the response of buildings during severe seismic events is considered.

## 7. Conclusion

Within the frame of the present paper, the Dyson and Bethe–Salpeter equation for the configurationally averaged field and field correlation are applied to study the change of the seismic site response by the presence of a city. The buildings are modelled as resonant scatterers that are uniformly distributed at the surface of a deterministic, horizontally layered elastic half-space that represents the soil. The distribution of the resonance frequencies of the buildings is estimated from the distribution of the number of floors of the buildings.

The approximate solutions of the Dyson and Bethe–Salpeter equation are used to study the site response due to a vertically incident SH wave for the case of Mexico City. In this particular case, the resonance frequencies of the buildings are higher than the first site resonance frequency.

The effect of the city on the site response in this case is twofold. First, the mean or coherent site response is modified. The mass of the buildings shifts the first site resonance frequency to a lower value. Second, the presence of the city induces a spatial variability of the site response. The multiple wave scattering that results from the interaction of the buildings and the soil shifts a part of the energy of the coherent field to the incoherent field component. The incoherent field is relatively small, however, and the resonant multiple wave scattering would only play an important role in the seismic response of a city if the buildings act as lossless scatterers. The solution is in close agreement with results from a numerical model of a city quarter of limited size that fully accounts for multiple wave scattering between a large number of buildings.

## Appendix A: Power balance for the scattering on a single building

The general power balance for the scattering on a single building is derived here from the field equation (1) in the case of a single building $\Omega_b$ resting on a purely elastic half-space $\Omega$. Multiplying equation (1) by the conjugate of the velocity $-i\omega\overline{\mathbf{u}}$, integrating over $D = \Omega_b \cup \Omega$, integrating by parts and taking the real part reads:

$$\omega\Im\left(\int_{\Gamma_\infty} \mathbf{t}(\mathbf{u}) \cdot \overline{\mathbf{u}} dS - \int_D \{\sigma(\mathbf{u}) : \epsilon(\overline{\mathbf{u}}) - \rho\omega^2 \|\mathbf{u}\|^2\} dV\right) = 0 \tag{A1}$$

Since dispersion is only taking place inside $\Omega_b$, the imaginary part of the second term vanishes everywhere but on $\Omega_b$ for the inner forces. Moreover, writing $\mathbf{u}$ as the sum of the incident and the scattered field in the first term and noticing that:

$$\Im\left(\int_{\Gamma_\infty} \mathbf{t}(\mathbf{u}_i) \cdot \overline{\mathbf{u}}_i dS\right) = \Im\left(\int_{\Omega} \{\sigma(\mathbf{u}_i) : \epsilon(\overline{\mathbf{u}}_i) - \rho\omega^2 \|\mathbf{u}\|^2\} dV\right) = 0 \tag{A2}$$

gives the following power balance:

$$\underbrace{-\Im\left(\int_{\Gamma_\infty} \{\mathbf{t}(\mathbf{u}_d) \cdot \overline{\mathbf{u}}_i + \mathbf{t}(\mathbf{u}_i) \cdot \overline{\mathbf{u}}_d\} dS\right)}_{P_{\text{out}}/\omega = -P_{\text{in}}/\omega} = \underbrace{\Im\left(\int_{\Gamma_\infty} \mathbf{t}(\mathbf{u}_d) \cdot \overline{\mathbf{u}}_d dS\right)}_{P_{\text{d}}/\omega} \underbrace{-\Im\left(\int_{\Omega_b} \sigma(\mathbf{u}) \epsilon(\overline{\mathbf{u}}) dV\right)}_{P_{\text{a}}/\omega} \tag{A3}$$

where $P_{\text{in}}$ is the power brought by the incident field, $P_{\text{d}}$ is the power lost by scattering and $P_{\text{a}}$ is the power lost by absorption inside the building. Noticing now that $\Omega$ is purely elastic the reciprocity theorem shows that all these terms can be equivalently written on the soil–building interface $\Gamma$ with an outer normal convention for the soil:

$$P_{\text{out}} = \omega\Im\left(\int_{\Gamma} \{\mathbf{t}(\mathbf{u}_d) \cdot \overline{\mathbf{u}}_i - \overline{\mathbf{t}(\mathbf{u}_i)} \cdot \mathbf{u}_d\} dS\right) \tag{A4}$$

$$P_{\text{d}} = -\omega\Im\left(\int_{\Gamma} \mathbf{t}(\mathbf{u}_d) \cdot \overline{\mathbf{u}}_d dS\right) \tag{A5}$$

$$P_{\text{a}} = \Im\left(\int_{\Gamma} \mathbf{t}(\mathbf{u}) \cdot \overline{\mathbf{u}} dS\right) \tag{A6}$$

Once normalized by the power density of the incident field, $P_{\text{out}}$, $P_{\text{d}}$ and $P_{\text{a}}$ define the total, the scattering and the absorption cross-sections, respectively.

## References


[1] Chavez-Garcia, F. J. and Bard, P.-Y., 1994, Site effects in Mexico City eight years after the September 1985 Michoacan earthquakes. *Soil Dynamics and Earthquake Engineering*, **13**, 229–247.

[2] Singh, S. K., Mena, E. and Castro, R., 1988, Some aspects of source characteristics of the 19 September Michoacan earthquake and ground motion amplification in and near Mexico City. *Bulletin of the Seismological Society of America*, **78**, 451–477.

[3] Wirgin, A. and Bard, P.-Y., 1996, Effects of buildings on the duration and amplitude of ground motion in Mexico City. *Bulletin of the Seismological Society of America*, **86**, 914–920.

[4] Clouteau, D. and Aubry, D., 2001, Modification of the ground motion in dense urban areas. *Journal of Computational Acoustics*, **9**, 1659–1675.

[5] Guéguen, P., Bard, P.-Y. and Chavez-Garcia, F. J., 2002, Site–city seismic interaction in Mexico City-like environments: An analytical study. *Bulletin of the Seismological Society of America*, **92**, 794–811.

[6] Mezher, N., Clouteau, D. and Ishizawa, O., 2003, Modélisation numérique de l'intéraction multiple sols-structures. In M. Potier-Ferry, M. Bonnet, and A. Bignonnet (Eds), *Actes du Sixième Colloque National en Calcul des Structures*, pages 157–164, Giens, France, May 20–23. Ecole Polytechnique.

[7] Mezher, N., 2004, *Modélisation numérique et quantification de l'effet sismique Site-Ville*. PhD thesis, Laboratoire de Mécanique des Sols, Structures et Matériaux, Ecole Centrale de Paris.

[8] Tsogka, C. and Wirgin, A., 2003, Simulation of seismic response in an idealized city. *Soil Dynamics and Earthquake Engineering*, **23**, 391–402.
[9] Groby, J.-P., Tsogka, C. and Wirgin, A., 2005, Simulation of seismic response in a city-like environment. *Soil Dynamics and Earthquake Engineering*, **25**, 487–504.
[10] Boutin, C. and Roussillon, P., 2004, Assessment of the urbanization effect on seismic response. *Bulletin of the Seismological Society of America*, **94**, 251–268.
[11] Foldy, L. L., 1945, The multiple scattering of waves I. General theory of isotropic scattering by randomly distributed scatterers. *Physical Review*, **67**, 107–119.
[12] Waterman, P. C. and Truell, R., 1961, Multiple scattering of waves. *Journal of Mathematical Physics*, **2**, 512–537.
[13] Lagendijk, A. and van Tiggelen, B. A., 1996, Resonant multiple scattering of light. *Physics Reports*, **270**, 143–215.
[14] Frisch, U., 1966, La propagation des ondes en milieu aléatoire et les équations stochastiques. *Annales d'Astrophysique. Première Partie.*, **29**, 645–682.
[15] Frisch, U., 1967, La propagation des ondes en milieu aléatoire et les équations stochastiques. *Annales d'Astrophysique. II. Applications.*, **30**, 565–601.
[16] Rytov, S. M., Kravtsov, Y. A. and Tatarskii, V. I., 1989, *Principles of Statistical Radiophysics. Wave Propagation through Random Media*, Volume 4 (Berlin: Springer-Verlag).
[17] Sheng, P., 1998, *Introduction to Wave Scattering, Localization and Mesoscopic Phenomena* (New York: Academic Press).
[18] Weaver, R. L., 1997, Multiple-scattering theory for mean responses in a plate with sprung masses. *Journal of the Acoustical Society of America*, **101**, 3466–3747.
[19] Weaver, R. L., 1998, Mean-square responses in a plate with sprung masses, energy flow and diffusion. *Journal of the Acoustical Society of America*, **103**, 414–427.
[20] Clough, R. W. and Penzien, J., 1993, *Dynamics of Structures*, 2nd edn (New York: McGraw-Hill).
[21] European Committee for Standardization, 1998, *Eurocode 8: DEsign Provisions for Earthquake Resistance of Structures – PArt 1–4:GEneral Rules – STrengthening and Repair of Buildings*.
[22] Savin, E., 1999, *Influence de la variabilité spatiale en interaction sismique sol-structure*. PhD thesis, Laboratoire de Mécanique des Sols, Structures et Matériaux, Ecole Centrale de Paris.
[23] Savin, E. and Clouteau, D., 2002, Elastic wave propagation in a 3-D unbounded random heterogeneous medium coupled with a bounded medium. Application to seismic soil–structure interaction (SSSI). *International Journal for Numerical Methods in Engineering*, **54**, 607–630.
[24] Aubry, D. and Clouteau, D., 1992, A subdomain approach to dynamic soil–structure interaction. In V. Davidovici and R.W. Clough (Eds), *Recent advances in Earthquake Engineering and Structural Dynamics*, pages 251–272. Ouest Editions/AFPS, Nantes.
[25] Ishimaru, A., 1997, *Wave Propagation and Scattering in Random Media*. IEEE Press–Oxford University Press Classic Reissue.
[26] Kennett, B. L. N., 1983, *Seismic Wave Propagation in Stratified Media* (Cambridge: Cambridge University Press).
[27] Apsel, R. J. and Luco, J. E., 1983, On the Green's functions for a layered half-space. Part II. *Bulletin of the Seismological Society of America*, **73**, 931–951.
[28] Luco, J. E. and Apsel, R. J., 1983, On the Green's functions for a layered half-space. Part I. *Bulletin of the Seismological Society of America*, **4**, 909–929.
[29] Clouteau, D., 1999, *MISS Revision 6.2, Manuel Utilisateur*. Laboratoire de Mécanique des Sols, Structures et Matériaux, Ecole Centrale de Paris.
[30] Shapiro, N. M., Olsen, K. B. and Singh, S. K., 2002, On the duration of seismic motion incident on the valley of Mexico for subduction earthquakes. *Geophysical Journal International*, **151**, 501–510.
[31] Singh, S. K. and Ordaz, M., 1993, On the origin of long coda observed in the lake-bed strong-motion records of Mexico City. *Bulletin of the Seismological Society of America*, **83**, 1298–1306.